25

~~SECRET~~

MAY 28 1962

UNCLASSIFIED

NAA-SR-6561
COPY 64 OF 150
66 PAGES
SERIES A

MASTER

THERMAL DESIGN OF SNAP REACTORS

(Title Unclassified)

AEC Research and
Development Report

~~RESTRICTED DATA~~

~~This document contains restricted data as defined in the Atomic Energy Act of 1954. Its transmittal or the disclosure of its contents in any manner to an unauthorized person is prohibited.~~

ATOMICS INTERNATIONAL
A DIVISION OF NORTH AMERICAN AVIATION, INC.

UNCLASSIFIED

DISTRIBUTION OF THIS DOCUMENT IS UNLIMITED

~~SECRET~~

1 8250

DISCLAIMER

Printed in USA Price $1.30 Available from the

U. S. Atomic Energy Commission
Technical Information Extension,
P. O. Box 1001
Oak Ridge, Tennessee.

Please direct to the same address inquiries covering the procurement of other classified AEC reports.

DECLASSIFIED

~~SECRET~~

UNCLASSIFIED

NAA-SR-6561
SNAP REACTOR,
SNAP PROGRAM
M-3679 (25th Ed.)

Classification cancelled (or changed to UNCLASSIFIED
letter 4/17/73
by authority of Bram Feldman Div of Clas. Wash DC
by GG DTIE, date 5/24/73

Exempt from CCRP Re-review Requirements
(per 7/22/82 Duff/Caudle memorandum)
HR 7/8/04

THERMAL DESIGN OF
SNAP REACTORS
(Title Unclassified)

By

PAUL D. COHN

~~RESTRICTED DATA~~

~~This document contains restricted data as defined in the Atomic Energy Act of 1954. Its transmittal or the disclosure of its contents in any manner to an unauthorized person is prohibited.~~

ATOMICS INTERNATIONAL
A DIVISION OF NORTH AMERICAN AVIATION, INC.
P.O. BOX 309 CANOGA PARK, CALIFORNIA

DISTRIBUTION OF THIS DOCUMENT IS UNLIMITED
GG

CONTRACT: AT(11-1)-GEN-8
ISSUED: FEBRUARY 1, 1962

UNCLASSIFIED

~~SECRET~~

DECLASSIFIED

~~SECRET~~

DISTRIBUTION

Category: SNAP REACTOR, SNAP PROGRAM
M-3679 (25th Ed.)

	Copy No.
Advanced Research Projects Agency	1-2
Aeronautical Systems Division	3-5
Air Force Space Systems Division	6-10
Air Force Special Weapons Center	11-16
Air Technical Intelligence Center	17
Air University Library	18
Argonne National Laboratory	19
Army Ballistic Missile Agency	20
Atomic Energy Commission, Washington	21-25
Battelle Memorial Institute	26
Bureau of Naval Weapons	27-28
Bureau of Ships	29-30
Bureau of Yards and Docks	31
California Patent Group	32
Chicago Operations Office	33-34
Defense Atomic Support Agency, Sandia	35
Department of the Army	36-38
Director of Defense Research and Engineering (OABCW)	39
Jet Propulsion Laboratory	40-41
Los Alamos Scientific Laboratory	42
Naval Ordnance Laboratory	43-44
Naval Radiological Defense Laboratory	45
Naval Research Laboratory	46-47
New York Operations Office	48
Office of the Chief of Ordnance, DOFL	49
Office of the Chief of Naval Operations	50-52
Office of Naval Research	53-54
Rand Corporation	55
Rome Air Development Center	56
School of Aviation Medicine	57
Union Carbide Nuclear Company (ORNL)	58
University of California, Livermore	59
University of Pennsylvania	60-62
University of Washington, APL	63
Division of Technical Information Extension	64-98
AI Library (Includes 2 for CPAO)	99-150

~~SECRET~~

CONTENTS

FIGURES

I. INTRODUCTION

This report describes the analytical techniques used in the preliminary thermal design of the SNAP 8 and SNAP 2 reactors. These analytical procedures, which were used in the design point selection for the SNAP 8 Experimental Reactor (S8ER) and the SNAP 2 Experimental Reactor (S2ER), are applicable to most core designs which incorporate a close packed array of fuel rods (Figure 1).

Methods suitable for calculating the thermal performance of reactor cores are presented in Chapter II. Analytical procedures for predicting the thermal behavior of components external to the core such as the reflector and shield are described in Chapter III. Derivations of important equations used in the reactor thermal analysis are given in the Appendix.

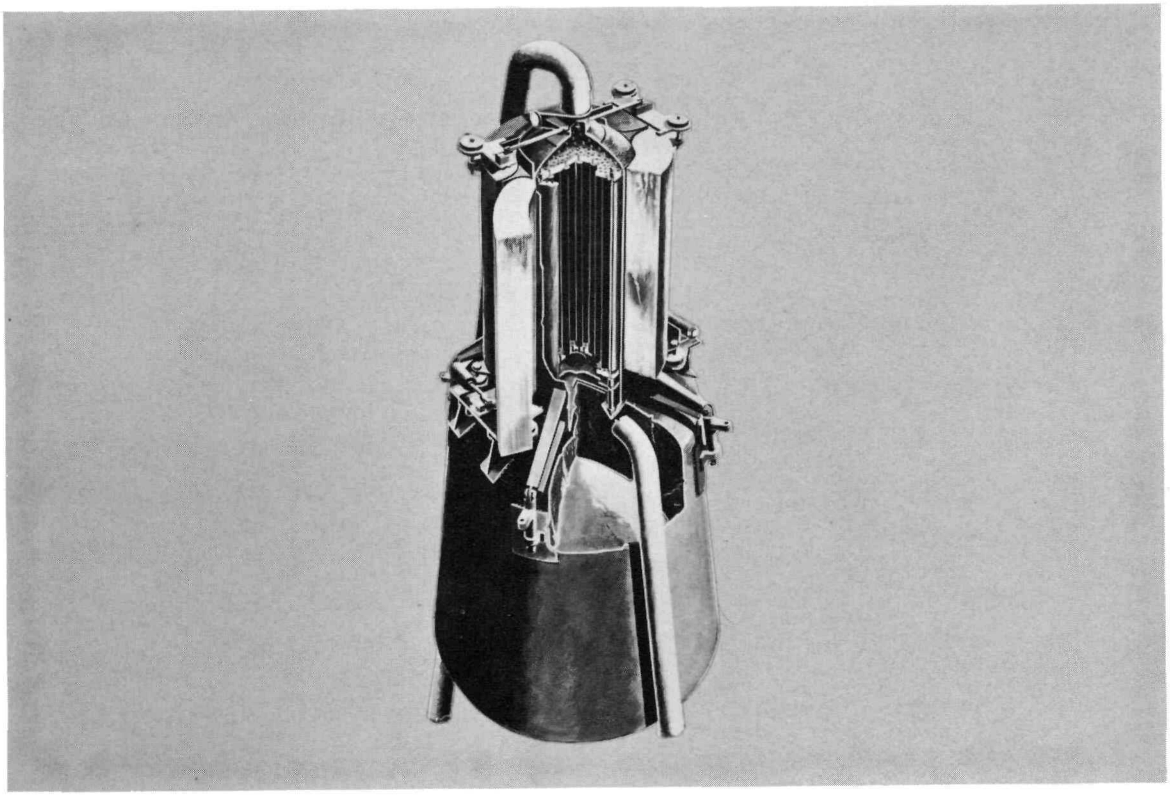

Figure 1. Typical SNAP Reactor

II. CORE THERMAL DESIGN

This chapter details the methods used to predict core temperatures, pressure drop, hydrogen loss, thermal stress, cladding creep, radiation damage effects, and hydrogen redistribution. When final design points are required, a parameter survey of number of fuel rods, diameter, spacing, and cladding along with a core parameter survey from both a thermal and nuclear standpoint must be performed.

A. DETERMINATION OF CORE THERMAL CONDITIONS

This section of the report outlines methods that may be used to predict the thermal conditions that would be present in the core. These include fuel temperatures, cladding and hydrogen barrier temperatures, coolant temperatures, and grid plate and internal reflector temperatures.

1. Thermal Design of Fuel Elements

Methods of estimating the thermal effects of the fuel element size; fuel element number; fuel element spacing; cladding, coating, and hydrogen gap; and radial flow distribution are included in this section. The final portion of this section demonstrates the combination of the various design considerations to produce the temperatures throughout the fueled portion of the core.

a. Fuel Element Diameter, Number

One of the major design considerations in any core is the size of the fuel elements. The fuel element diameter should be large enough to offer ease of fabrication and minimum non-fuel material in the core and, at the same time, be small enough so that the core temperature limitations are not exceeded.

The number of fuel elements in a hexagonal array in a core of given radius may be estimated[*] by

$$n = 0.83\,\epsilon_s \frac{R^2}{r^2} \qquad \ldots(1)^{\dagger}$$

---

[*] A drawing of the core must be made to determine if this number will fit conveniently in the hexagonal array.

[†] Standard nomenclature is given on Page 31.

where

$$\epsilon_s = \frac{0.906}{\alpha^2} \qquad \ldots(2)$$

α, the pitch to diameter ratio, is a significant parameter in determining the fuel element temperatures and will be discussed in some detail in the following subsection.

b. <u>Fuel Element Spacing</u>

Fuel element spacing has an important effect on the temperatures in the element. The spacing is usually denoted by α which is the distance between adjacent fuel rod centers divided by the fuel rod diameter. In cores with high power densities, greater than 1.5 Mw/ft^3, and coolant temperatures in excess of 1300°F, an insured α greater than 1.00 (rods do not touch) is usually necessary to reduce cladding and fuel temperatures. There are several methods of insuring an α greater than 1.00. This may be accomplished by wire wrapping the fuel elements, indexing the elements in the grid plates, or other raised surfaces on the cladding and/or end caps.

Figures 2 and 3 demonstrate the effect of α on the effective heat transfer area for the cladding, coating, and hydrogen gap (Figure 2) and the fuel rod temperature drop (Figure 3).

The normal temperature drop[*] across the fuel rod, ΔT_{fo}, may be calculated by,

$$\Delta T_{fo}(R, Z) = \frac{Q(R, Z) r^2}{4k_f} \qquad \ldots(3)$$[†]

where

$$Q(R, Z) = \frac{P(R, Z)}{\epsilon_f V_c} \qquad \ldots(4)$$

---

[*] The normal temperature drop is defined as the temperature drop in a bare rod with uniform heat generation immersed in a coolant of infinite extent.

[†] Appendix A (Part I).

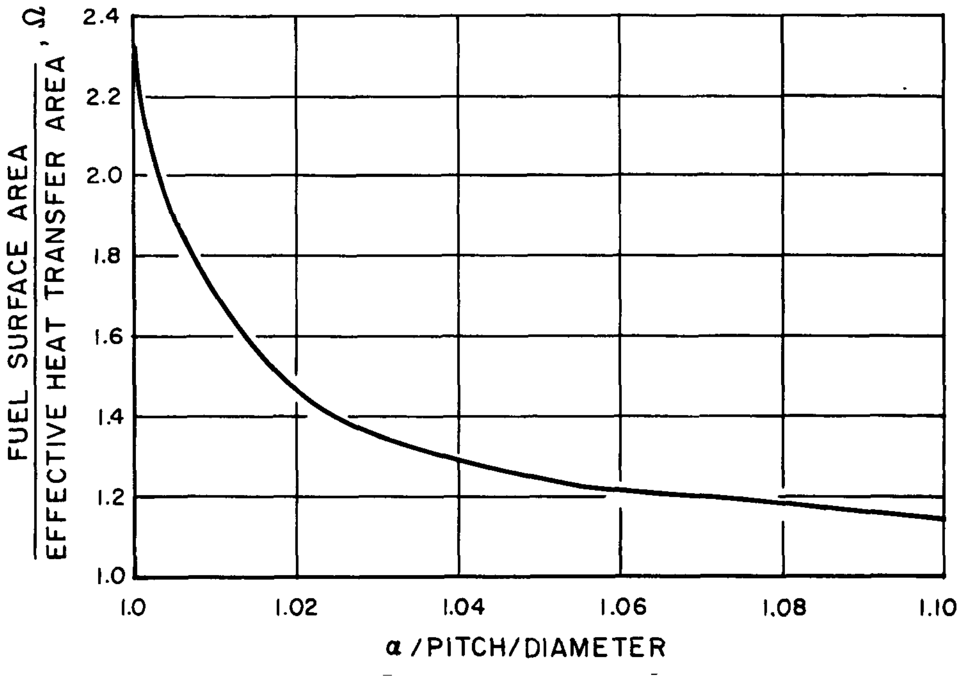

Figure 2. Effective Heat Transfer Area for Cladding, Coating, Hydrogen Gap, and Coolant Film

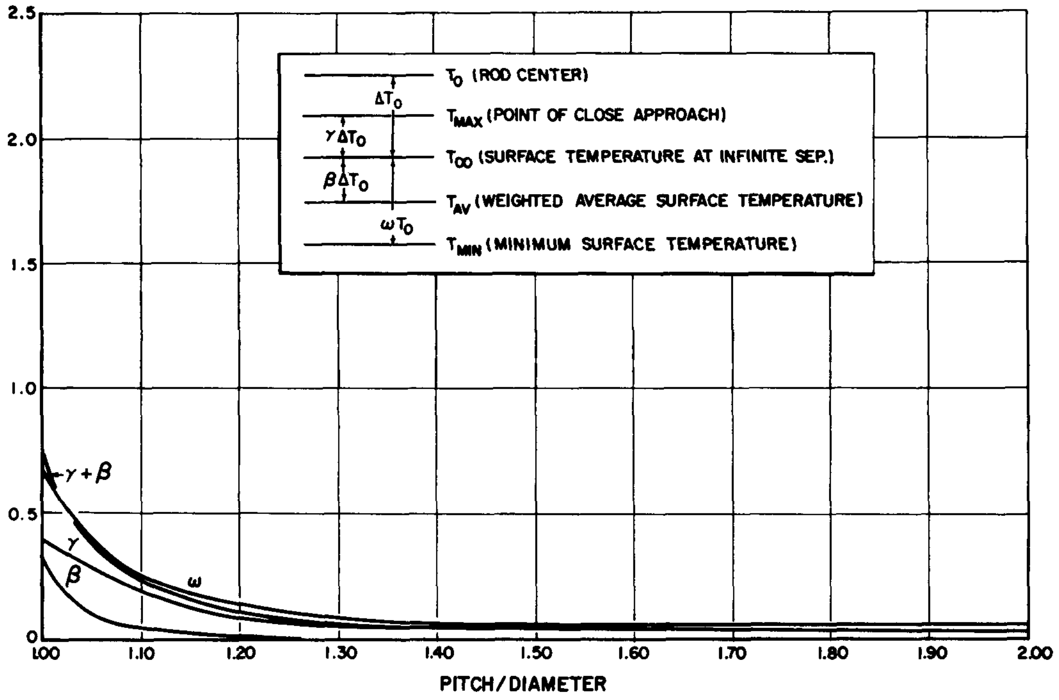

Figure 3. Parameters for Tricusp Channel Turbulent Flow[9,10]

P(R, Z) is the reactor power as a function of the reactor radius, R, and length, Z. The power distribution is considered to be separable into its radial and axial components; i.e., P(R, Z) is a function of R only at constant Z and conversely P(R, Z) is a function of Z only at constant R. In SNAP reactors the radial power distribution has the shape of a chopped cosine function with a peak/average variation of about 1.3 and a peak/minimum variation of about 1.7. The axial peak/average and peak/minimum variations which have a shape similar to the radial distribution are about 1.4 and 3.5 respectively.

In some reactor designs flow shaping (Subsection d) and/or the various thermal modifications mentioned in this part may not be adequate in producing optimum thermal conditions in the core due to size restrictions, etc. If this is the case, power flattening may be considered. Power flattening is accomplished by several methods all of which tend to increase the core volume as the removal of fuel or moderating material from a high importance region is usually involved. Radial power flattening may be obtained by radial variations in N_H, uranium loading, or fuel rod diameter. To some extent the change in core volume due to the methods mentioned above is compensated by an increase in reflector worth at the core periphery. Axial power flattening may be accomplished by variation of the hydrogen or uranium concentration axially in the fuel elements.

c. Cladding and Coating Effects

The fuel elements in SNAP reactors are clad in order to contain fission products as well as protect the fuel material from the coolant. In addition, the cladding is coated on the inside with a ceramic material that reduces hydrogen moderator loss. As pointed out previously in Subsection b, the fuel element separation should be considered in cladding design. Figure 2 demonstrate the area reduction due to close packing.[1,2] An added consideration in the cladding and coating temperatures is the hydrogen gap between the fuel surface and the hydrogen barrier (coating). Shrink fitting or thermal bonding of the cladding to the fuel are methods of eliminating the temperature rise due to the hydrogen gap.

The methods of calculating the normal temperature drops* through the hydrogen gap, coating, and cladding are given on the following page.

---

*Normal temperature drop is defined as that temperature drop that will be present in an element with uniform heat flux over the face considered.

Hydrogen gap:

$$\Delta T_{Ho}(R, Z) = \frac{P(R, Z)X_H}{nA_f k_H} \qquad \ldots(5)$$

if $X_H << r$

Coating:

$$\Delta T_{so}(R, Z) = \frac{P(R, Z)X_s}{nA_s k_s} \qquad \ldots(6)$$

if $X_s << r$

Cladding:

$$\Delta T_{co}(R, Z) = \frac{P(R, Z)X_c}{nA_c k_c} \qquad \ldots(7)$$

if $X_c << r$

The temperature drop through the coolant film if the coolant is a liquid metal is given by Equation 8

$$\Delta T_{mo}(R, Z) = \frac{P(R, Z)}{nA_c h_m} \qquad \ldots(8)$$

$$h_m{}^{(1)} = 0.625 \frac{k_m}{D_e}\left(\frac{GD_e C}{k_m}\right)^{0.4} \qquad \ldots(9)$$

where

$$D_e = \left(\frac{1}{\epsilon_s} - 1\right) D \qquad \ldots(10)$$

and G is the mass flow rate per coolant channel.

d. Thermal Considerations of Coolant Flow

The radial distribution of coolant flow is an important consideration in SNAP core design in that several thermal characteristics of the core may be modified by choice of a particular flow distribution. Some thermal changes resulting from flow profile modifications are 1) reduction of reactivity loss due to hydrogen leakage from high importance regions, 2) reduction of maximum cladding, coating, and fuel temperatures, 3) minimizing hydrogen redistribution effects, 4) reduction of thermal stress damage, and 5) reduction of temperature induced radiation damage and cladding creep. Most of the above are temperature and temperature gradient dependent and the thermal limits and degree of severity of each must be known in order to determine which controls the selection of the radial flow distribution. The optimum flow distribution may be predicted by use of Equations 13, 14, and 15 along with the necessary experimental and calculated information concerning hydrogen loss, fuel strength, etc.

e. Hot Channel Factors

The application of hot channel factors is important in SNAP core design particularly in applications where the core power density is high and thermal limitations are severe. In general hot channel factors include the effects of fuel loading accuracy, fuel N_H tolerances, accuracy in predicting power distribution and variation during core life, variations in the flow distribution, and core design tolerances. In SNAP reactors, the last item is usually not included as both the nuclear and thermal designs are based on the most severe mechanical tolerances for each case.

The N_H and fuel loading variations may be estimated by reference to fuel composition data for cores with similar N_H and uranium loadings. The N_H variation and the uranium variation are about the same for N_H 5.5-6.5 and uranium 5 to 10 wt % and are usually ±5% for each. The accuracy of predicting the power distribution and variation during the core life may be determined from the nuclear design calculations and a knowledge of the reflector movements during the reactor life. The flow variation from ideal flow may be determined from the core hydraulic experiments; these are discussed in a following subsection. A reasonable limitation on the flow accuracy is ±10%, although this variation may not be tolerable for high power densities.

The increased temperature rise due to hot channel factors in the fuel, hydrogen gap, coating, cladding, and coolant film may be found by the product of the individual hot channel factors times the respective temperature rises,

$$\Delta T_{ht.\,ch.} = I_f I_{N_H} I_P \Delta T_o \quad . \qquad \ldots(11)$$

The axial temperature rise increase along a coolant channel due to the hot channel effects may be found by:

$$\Delta T_{m,\,ht.\,ch.\,(axial)} = \Delta T_{mo(axial)} I_f I_{N_H} I_P I_m \qquad \ldots(12)$$

where $\Delta T_{mo(axial)}$ is the second term on the right side of Equation 13. It should be noted that the hot channel effect is considered to be the worst thermal condition in the core; thus the final hot channel factor is the product of all the individual hot channel factors.

f. Estimation of Core Temperatures

(1) Coolant Temperature

The bulk coolant temperature in a coolant channel at a constant reactor radius R, with a flow rate m(R), may be calculated by:

$$T_m(R, Z) = T_i + \frac{1}{2} \, \frac{\int_0^Z P(R, Z)dZ}{m(R)C_m L} \quad . \qquad \ldots(13)$$

(2) Cladding and Coating Temperatures

The maximum cladding and coating temperatures at a particular core height occur at the point of closest element approach and are for all purposes the same, as the point of closest approach tends to be adiabatic. The maximum cladding and coating temperature at a reactor radius R and height Z may be calculated using the normal temperature drops and close packing effects described in previous subsections by:

$$T_{c,\,s_{max}}(R,Z) = T_m(R,Z) + \Omega^{\dagger}\Delta T_{mo}(R,Z) + \Omega\Delta T_{co}(R,Z) + \Omega\Delta T_{so}(R,Z) + \Omega\Delta T_{Ho}(R,Z) + (\gamma+\beta)^{\dagger\dagger}\Delta T_{fo}(R,Z). \quad \ldots(14)$$

The derivations of the quantities γ, β, and Ω are given in Appendix A, Parts I, II, and III.

(3) Fuel Temperatures

The maximum fuel surface temperature may be assumed to be the same as $T_{c,\,s_{max}}$; the fuel center line temperature at a reactor radius R, and core height Z may be calculated by:

$$T_{f_{max}}(R,Z) = T_{c,\,s_{max}}(R,Z) + (1-\gamma)\Delta T_{fo}(R,Z). \quad \ldots(15)$$

If hot channel factors are used in the thermal analysis, the various temperature rises described by Equations 13, 14, and 15 should be multiplied by the hot channel factors, the application of which is outlined in Subsection e.

2. Thermal Design of Other Core Members

a. Internal Reflectors

Internal reflectors attached to the core perimeter require little consideration from a thermal standpoint as they usually consist of materials with high thermal conductivity and temperature stability such as Be, BeO, and Ni. If the internal reflectors consist of low thermal conductivity materials or have fuel loading, an estimate at the thermal conditions in these components should be made. An analysis similar to that conducted for the fuel elements would be adequate. The heat generation due to gamma and neutron attenuation in these materials is discussed in Chapter III of this report.

b. Grid Plates

The grid plates normally have no thermal limitations since the fuel rods generally have much more stringent thermal requirements. The basic

---

†Figure 2

††Figure 3

consideration for the design of the grid plates is that they be adequate to support the core during the launch phase when the system is cold.

An important consideration in the integral reactor design is that the extreme stress and vibration during the launch phase not cause damage to the core, and that when the core temperature rises at startup the fuel rods are free to expand. These may be accomplished by constructing the vessel and grid plates with materials that have a higher thermal expansion coefficient than the fuel. Thus a cold core may be a tight package at the launch phase, but will allow fuel rod expansion as the core temperature rises.

B. COOLANT FLOW

The selection of the flow rate and reactor inlet and outlet temperatures are dependent on the power level of the core and the thermodynamic characteristics of the power conversion system and radiator. This section presents a summary of flow profile considerations, methods of predicting core pressure drop, and the role of core mockup hydraulic experiments in core design.

1. Flow Profile

The flow profile as discussed in Section A-d, should be known in order to determine core temperature, hydrogen loss, etc. Where thermal problems in the core may be eased by the proper choice of radial flow profile, the use of a modified inlet plenum area may be necessary to insure the flow shape required. The optimum flow configuration may be determined by an iterative solution of Equation 13 when the various thermal limitations of the core, such as cladding temperature, hydrogen containment, and thermal stress are known. In any case, a hydraulic flow model is necessary to determine that maldistribution of coolant does not exist and that the core receives adequate coolant throughout. The use of hydraulic models is discussed in Subsection 3.

2. Pressure Drop

The pressure drop through the core may be calculated in the following manner:[3]

a. Core Inlet

$$\Delta p = \frac{\rho V_1^2}{288 g_c}\left(1 - \frac{S_1}{S_2}\right)^2 \text{ (psi)} \qquad \ldots(16)$$

where

V_1 = the velocity in the entrance pipe

S_1 and S_2 = the inlet pipe area and the lower plenum cross section respectively.

b. Lower Grid Plate

(1) Entrance

$$\Delta p = \frac{K V_2^2 \rho}{288 g_c} \text{ (psi)} \qquad \ldots(17)$$

where V_2 is the velocity in the grid plate and $K = 0.5$ for most cases.

(2) Channel

The standard drag equation may be used for this calculation:

$$\Delta p = \frac{f \rho V_2^2 \ell_2}{288 D g_c} \text{ (psi)} \qquad \ldots(18)$$

where ℓ_2 = the channel length.

(3) Exit

$$\Delta p = \frac{\rho V_2^2}{288 g_c}\left(1 - \frac{S_2}{S_3}\right) \text{ (psi)} \qquad \ldots(19)$$

where S_2 is the channel area and S_3 is the tricusp area between the fuel rods.

c. Fuel Channel

$$\Delta p = \frac{f W \rho V_3^2 \ell_3}{288 D_e g_c} \text{ (psi)} \qquad \ldots(20)$$

where

D_e is defined by Equation 10

V_3 = velocity in the fuel channel

ℓ_3 = the fuel rod length

W = 1.0 for bare fuel rods and $\left(1 + \frac{\pi D}{\theta}\right)^{2.78}$ for wire wound fuel rods (θ = the wire pitch).

d. Top Grid Plate

(1) Entrance

$$\Delta p = \frac{K \rho V_4^2}{288 g_c} \text{ (psi)} \qquad \ldots (21)$$

where

V_4 = the coolant velocity in the upper grid plate

and

$K = 0.4\ (1.25 - S_4/S_3)$

for

$S_4/S_3 < 0.715$

or

$K = 0.75\ (1 - S_4/S_3)$

for

$S_4/S_3 > 0.715$

where

S_4/S_3 = ratio of the grid plate channel area to the tricusp fuel channel area.

(2) Channel

Equation 18 may be used.

(3) Exit

$$\Delta p = \frac{\rho V_4^2}{288 g_c}\left(1 - \frac{S_4}{S_5}\right)^2 \text{ (psi)} \qquad \ldots(22)$$

where

$\frac{S_4}{S_5}$ = the ratio of the grid plate channel area to the upper plenum cross section.

e. Core Vessel Exit

$$\Delta p = \frac{\rho K V_6^2}{288 g_c} \text{ (psi)} \qquad \ldots(23)$$

where

V_6 = coolant velocity in the outlet pipe

and

$K = 0.4\ (1.25 - S_6/S_5)$

for

$S_6/S_5 < 0.715$

and

$K = 0.75\ (1 - S_6/S_5)$

for

$S_6/S_5 > 0.715$

where

S_6/S_5 = the ratio of the upper plenum cross section to the outlet pipe area.

The total pressure drop through the core is the sum of the pressure drops described above.

3. Core Hydraulic Experiments

The use of core mockup hydraulic experiments in SNAP reactor thermal design is necessary to accurately predict the radial distribution of coolant flow (Subsection A-d). The usual procedure is to construct a dimensionally identical core consisting of simulated fuel rods which are instrumented to detect coolant flow rates. The flow rates are determined by injecting a salt solution into the upstream side of the core and recording the change in electrical conductivity of the water as the salt interface passes the instrumented fuel rod. The instrumented fuel elements are equipped with electrical probes at the top and bottom so that the flow rate in the individual channel may be determined. In some cases the flow mockup core is equipped with movable upper and lower plenum areas so that these areas may be modified by use of baffle plates, etc. to produce the required flow profile.

The Reynolds analogy is used to determine the water flow required for dynamic similarity with the NaK. The table below demonstrates this method.

$$\left(\frac{DV\rho}{\mu}\right)_{\text{model}} = \left(\frac{DV\rho}{\mu}\right)_{\text{reactor core}}, \qquad \ldots (24)$$

The following table may be constructed:

Dimension	H_2O Model	Reactor Core (NaK)	Comments
Characteristic dimension, D-ft	Same	Same	Usually the fuel channel, D_e
Velocity, V-ft-sec	Measured	Unknown distribution	The average velocity required in the model is determined by the average NaK velocity for the core.
Density, ρ-lb_m/ft^3	Known	Known	Evaluated at average thermal conditions
Viscosity, μ-lb_m/ft-sec	Known	Known	Evaluated at average thermal conditions

Similarly, the Euler equation may be applied to determine or check the pressure drop:

$$\left(\frac{\Delta p g_c}{\rho V^2}\right)_{\text{model}} = \left(\frac{\Delta p g_c}{\rho V^2}\right)_{\text{reactor core}}, \qquad \ldots(25)$$

and the following table may be constructed:

Dimension	H_2O Model	Reactor Core (NaK)	Comments
Pressure drop, Δp-lb_f/ft^2	Measured	Unknown	--
Velocity, V-ft/sec	Measured	Calculated or ideal	The velocity may be calculated from Equation 24
Density, ρ-lb_m/ft^3	Known	Known	Evaluated at average thermal conditions.
Gravity constant, $g_c \dfrac{lb_m\text{-}ft}{lb_f\text{-}sec^2}$	32.2	32.2	--

C. HYDROGEN MODERATOR

SNAP fuel elements are clad in order to impede the degradation of reactivity due to loss of the hydrogen moderator from the fuel as well as to protect the fuel from the coolant. The fuel rod cladding is coated on the inside with a ceramic material that greatly reduces the diffusion of the hydrogen through the cladding. This section presents methods of predicting the hydrogen leakage in SNAP cores, and a method of estimating the extent of hydrogen moderator redistribution in the fuel.

1. Hydrogen Loss

The hydrogen loss throughout the life of the core may be calculated by the following methods:

$$\%L_H = \frac{200tS_o}{Nr}\left(\frac{p}{1+ap}\right)\int_0^1 e^{-\bar{\Delta}E/T}\, d\left(\frac{Z}{L}\right) \qquad \ldots(26)^{\dagger}$$

---

†See Appendix B for the derivation of the hydrogen loss equations.

where

T = average coating temperature, °R

r = fuel rod radius, cm

p = internal fuel rod hydrogen pressure evaluated at the average fuel temperature in that region, atmospheres

$\frac{Z}{L}$ = the normalized axial coordinate.

The other terms are standard and are given in the nomenclature, Page 31.

Equation 26 should be used where the hydrogen loss throughout the core must be known accurately. It may be evaluated by numerical integration for several radial core zones depending upon the accuracy desired and the core radial temperature distribution. Recent investigations have given the following values for the constants in the equation.[1]

S_o = 10^5 cc/hr cm^2 atm for 4 coats of Solaramic

a = 0.15

$\bar{\Delta} E$ = 33,200

It should be noted that the blend at the welded end of the fuel element often has a leak rate as high as the cladding wall. Recent data have indicated that the leak rate temperature and pressure dependence at the blend is different than that for the tube wall. Blend leak rates are factored into the wall leak rate on an empirical basis.

For lower power cores, or where hydrogen loss is not an important parameter, the axial temperature rise may be assumed to be linear and Equation 26 may be integrated to give:

$$\%L_H = \frac{200 t S_o \bar{\Delta} E}{\Delta T}\left(\frac{p}{1 + ap}\right)\left[e^{-\mu}\left(\sum_{n=1}^{\infty} \frac{(-1)^n\, n!}{\mu^{n+1}}\right)\right]_{\mu = \frac{\bar{\Delta} E}{T_i}}^{\mu = \bar{\Delta} E/(T_i + \Delta T)} \qquad \ldots(26)$$

where ΔT is the integral of the third term in Equation 13 and is simply the core axial temperature rise. If ΔT is 200°F, the first 3 terms of the series in Equation 26 gives about 95% accuracy.

As was noted the internal fuel rod hydrogen pressure used in Equations 25 and 26 should be the pressure in the rod due to the average fuel temperature. This is because the hydrogen moderator in each fuel rod redistributes after the reactor has come to power and temperature such that its concentration at any rod point is that which gives the same hydrogen pressure as any other point in that fuel rod.

Flow shaping is a possible method of reducing hydrogen loss in the high-importance central region of the core. A trial and error approach is necessary to predict the proper flow shape to produce a minimum overall core reactivity loss from hydrogen leakage. When the radial variation of hydrogen reactivity worth is known for the particular core, a flow shape may be predicted by use of the equations outlined in Section A to predict coating temperatures that will give a minimum reactivity loss when these temperatures are used in the numerical integration of Equation 26.

2. Hydrogen Redistribution

The extent of hydrogen redistribution in a SNAP fuel rod may be calculated from Equation 27:

$$\frac{\Delta N}{N_o} = -\frac{Q^{\#}\Delta T}{RT_{av}^{2}} \qquad \ldots(27)^{\dagger}$$

where

$\frac{\Delta N}{N_o}$ = the fractional change in hydrogen concentration

$Q^{\#}$ = the heat of transport, cal/mole

ΔT = the temperature difference between the two points in question, °C

R = the universal gas constant, 1.987 cal/g mole-°K

T_{av} = the average temperature of the points in question, °K

---

†See Appendix B for derivation.

The value of $Q^{\#}$ for ZrH at temperatures between 1000°F and 1300°F for the normal redistribution times (~1000 hours) determined experimentally for SNAP fuels is about 900 cal/mole.[4]

D. OTHER THERMAL EFFECTS

This section gives methods of estimating the effects of radiation damage, cladding creep, and thermal stress. It should be noted that these areas do not now represent serious design problems; but as both core temperatures and power are increased in new reactor designs, the following will become significant in design considerations.

1. Radiation Damage

Permanent damage in SNAP fuel may take place in the form of cracking or swelling because of the pressures developed due to the formation of nonsoluble fission gases. The maximum fractional change in fuel rod volume, δ, may be estimated by Equation 28.[1,6]

$$\delta = 0.75 \frac{RmfT}{Y(T)}^{\dagger} \qquad \ldots(28)$$

where

m = gram moles of gas produced per fission

R = the universal gas constant

T = maximum fuel rod temperature, °R

f = the maximum fissions per cc during the reactor life

$Y(T)$ = the ultimate tensile strength of the fuel at temperature T.

Equation 28 is valid for high N_H SNAP fuels as these may be assumed to be perfectly brittle. Equation 28 is further restricted in that it holds only for small volume changes.

A certain amount of radiation damage to beryllium could be expected due to the formation of α particles from the n,α reactions in beryllium. Figure 4 demonstrates the effect that the integrated fast neutron dose and beryllium temperature has on Be swelling from this radiation.[5]

---

†Appendix C, Part I.

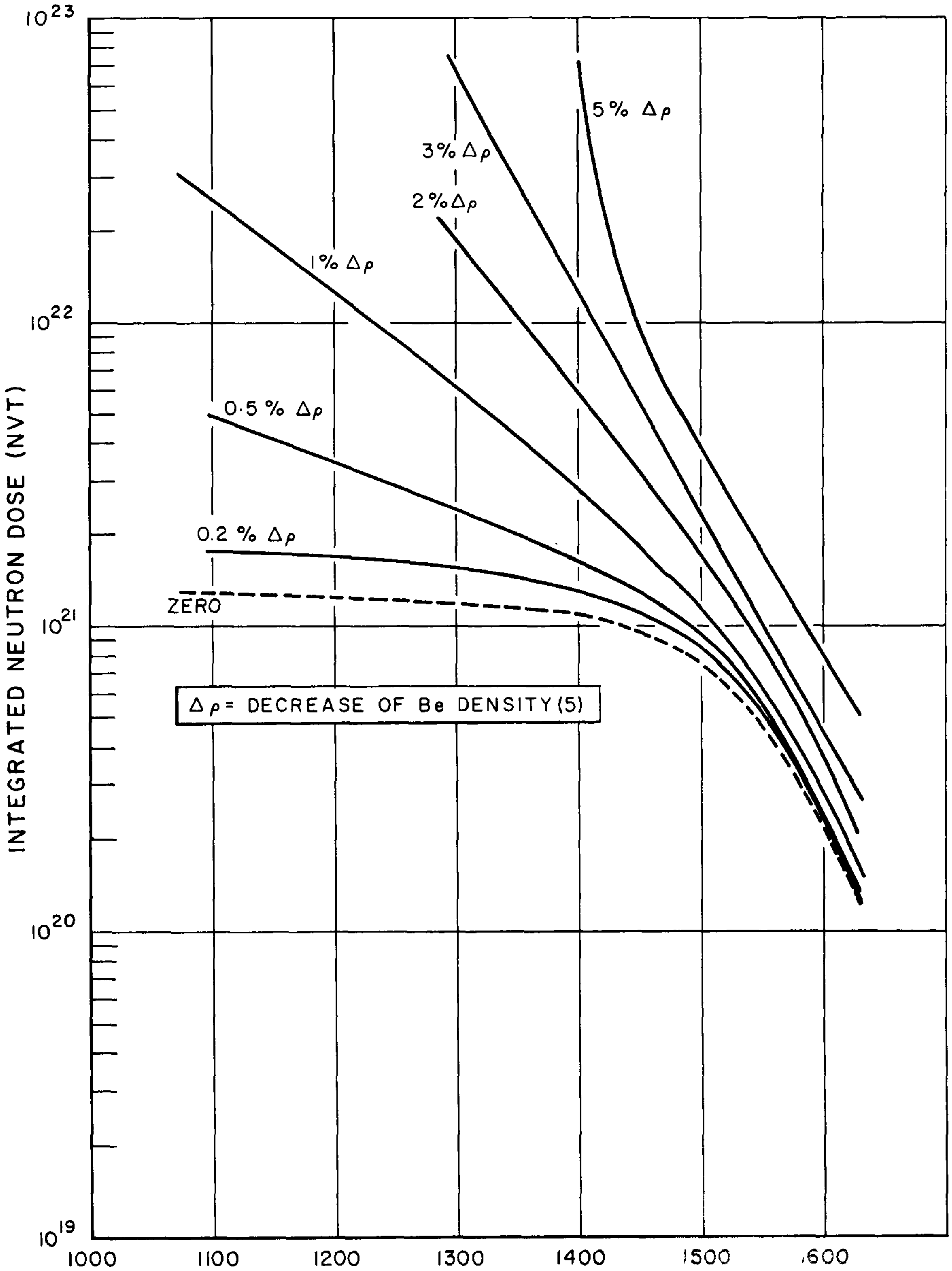

Figure 4. Radiation Damage in Beryllium

2. Thermal Stress

The thermal stresses developed in a SNAP fuel rod would be expected to crack the fuel if these stresses exceeded the ultimate tensile strength of the fuel material. It is not necessarily obvious that a cracked fuel element would not function properly in the core as long as the cladding remained integral. It could be assumed that a cracked fuel rod might have impaired heat transfer characteristics and the combination of a surface crack and continued thermal cycling could conceivably cause failure of the hydrogen barrier.

The maximum thermal stress in a fuel rod is normally in the axial direction and may be calculated by Equation 29.†

$$\sigma_{ZZ_{max}} = - E\alpha\gamma_o r^2 \left(1 + \omega + \frac{1}{2(1 - \nu)}\right) \qquad \ldots(29)$$

where

$\gamma_o = \frac{Q_{max}}{4k}$

α = the thermal expansion coefficient

ω = a function of the P/D ratio, α, is given in Figure 3.

3. Cladding Creep

In some cores where a combination of high N_H and high fuel temperature leads to a large internal fuel rod pressure, cladding creep may present a thermal problem. In particular where shrink fitting is used to reduce fuel and cladding temperatures, creep in the cladding has the effect of destroying the advantages gained by shrink fitting.

The stress developed in the cladding due to internal fuel element pressure is:

$$\sigma = \frac{(P - P_o)D}{2t} \qquad \ldots(30)$$

---

†See Appendix C, Parts I and II for the derivation of these equations.

where

σ = stress, psi

P = internal fuel rod pressure, psi

P_o = reactor operating pressure, psi

D = fuel element diameter, in.

t = cladding thickness, in.

P, the internal fuel rod pressure, is time dependent because of hydrogen redistribution (Section C). When the time dependence of P is known, the time function of σ may be calculated from Equation 30; with this information and the creep characteristics of the cladding material, the creep expected during the core life may be calculated.

III. THERMAL DESIGN OF COMPONENTS EXTERNAL TO THE CORE

Often thermal analyses of devices attached to or close to the reactor core are necessary because of the thermal conditions imposed on these components by radiation and temperature level.

A. REFLECTOR TEMPERATURES

The selection of the reflector material is often predicated on the temperature that the element will experience during operation. The temperature distribution as well as the maximum temperatures in the reflectors should be known to facilitate the design and selection of the reflector configuration. The reflector temperatures at core height Z may be calculated by a digital or analog solution of the equations given below:

Heat transfer at the reactor-reflector interface at any axial interior node n:

$$Q_{in} = \sigma \epsilon_i A_i (T_{in}^4 - T_{Bn}^4) + h_g A_i (T_{in} - T_{Bn}) \qquad \ldots(31)^{\dagger}$$

Axial and radial conduction in the reflector at any axial interior node n:

$$Q_{Bn}^{\dagger\dagger} + Q_{in} = \frac{k}{x} A(T_{Bn} - T_{on}) + n \frac{k}{Z} \frac{Az}{2} \left(2T_{Bn} - T_{B(n+1)} - T_{B(n-1)}\right) \qquad \ldots(31a)$$

Heat loss from the reflector exterior surface at any axial interior node n (to atmosphere or space):

$$\frac{k}{x} A(T_{Bn} - T_{on}) = \sigma \epsilon_o A_o (T_{on}^4 - T_A^4) + n \frac{k}{Z} \frac{Az}{2} \left(2T_{on} - T_{o(n-1)} - T_{o(n+1)}\right)$$

$$+ C_H A_o (T_{on} - T_A)^{1.25} . \qquad \ldots(31b)$$

---

†See Appendix D for the development of these equations.
††This quantity is also developed in Appendix D.

where

Q_i = the thermal radiation heat transferred from the reactor vessel to the reflector, Btu/hr

Q_B = nuclear radiation heat rate, Btu/hr

σ = Stefan-Boltzman constant 1.73×10^{-8} Btu/hr-ft^2(°R)^4

ϵ_i = emissivity at interface

ϵ_o = emissivity at beryllium surface

T_i = reactor coolant temperature at the core edge, °R

T_B = beryllium temperature at interface, °R

T_o = exterior beryllium temperature, °R

T_A = atmosphere or space temperature, °R

A_i = area at reactor vessel reflector interface, ft^2

A = average area for heat conduction through beryllium, ft^2

A_o = area at reflector exterior, ft^2

k = thermal conductivity of beryllium, Btu/hr-ft-°F

x = beryllium thickness, ft

h_g = gas heat transfer coefficient at reflector-reactor interface, Btu/hr-ft^2-°F

Z = node length in beryllium, ft

Az = annular area of beryllium cross section, ft^2

$C_H{}^{(3)}$ = gas heat transfer coefficient at reflector exterior surface - $\dfrac{\text{Btu}}{\text{hr-ft}^2\text{-°F}^{1.25}}$

n = number of nodes

B. SHIELD TEMPERATURE ESTIMATION[1]

As in the case of the reflectors, the shield has definite temperature limitations. In the case of a shield where the radiation input causes excessive heat generation leading to severe temperatures, certain modifications to the shield will allow reduction of these high temperatures. Where a LiH shield is used, usually heat generation in the first few inches is extremely high due to the immediate capture of the thermal leakage. A thin borated plate between the shield and reactor would eliminate the superfluours thermal flux and possibly make the temperatures acceptable. The use of a heavy "thermal" shield between the shield and the reactor has the effect of reducing the gamma flux. The secondary gamma generation due to neutron capture in these shields make them of limited value as most heavy, high temperature materials applicable for gamma attenuation generate these secondary emanations when bombarded with neutrons. The most effective thermal shield to use in conjunction with a LiH neutron shield is a heavy metal hydride with boron addition. This shield attenuates gammas as well as moderates neutrons along with complete blockage of the thermal leakage and neutrons thermalized in this shield. Boron has the additional advantage of forming only α particles upon capture of neutrons, thus reducing any radiation leakage from the thermal shield from this source.

Equations 32, 33, and 34 give a method of determining the temperatures at the centerline and edge of a shield which is radiating its heat to space or other heat sink. The equations are written for any intermediate point in the shield, but may be applied to shields of several materials by use of the appropriate boundary conditions as outlined in Appendix D, Part III.

If the shield is divided into nodes consisting of discs under the thermal shield, and rings consisting of the volume between the thermal shield and the perimeter, we may write a heat balance around node n; for heat generated in, conducted axially into and out of, and conducted radially to the perimeter of node Cn, and to the surface Sn under the thermal shield:

$$Q_{oc} r_{Bn} Z_n e^{-\mu Z_n (n-1)} = 4 k_n Z_n (T_{Cn} - T_{Bn}) + \frac{2 r_{Bn}^2 \left(T_{Cn} - T_{C(n-1)}\right)}{\frac{Z_{n-1}}{k_{n-1}} + \frac{Z_n}{k_n}}$$

$$+ \frac{2 r_{Bn}^2 \left(T_{Cn} - T_{C(n+1)}\right)}{\frac{Z_{n+1}}{k_{n+1}} + \frac{Z_n}{k_n}} \qquad \ldots (32)^{\dagger}$$

---

†See Appendix D, Part III for the development of these equations.

In the ring outside the thermal shield:

$$mQ_{oc}Z_n\left(r_{Sn}^2 - r_{Bn}^2\right) e^{-\mu Z_n(n-1)} = \frac{Z_n\left(mr_{Sn}^2 + r_{Bn}^2(1 - m)\right)\left(T_{Bn} - T_{Sn}\right)}{\frac{m}{4k_n}\left(r_{Sn}^2 - r_{Bn}^2\right) + \frac{r_{Bn}^2}{2k_n}(m - 1)\,\ell n\,\frac{r_{Bn}}{r_{Sn}}}$$

$$+ \frac{\left(r_{Sn}^2 - r_{Bn}^2\right)\left(T_{Bn} + T_{Sn} - T_{B(n-1)} - T_{S(n-1)}\right)}{\frac{Z_{n-1}}{k_{n-1}} + \frac{Z_n}{k_n}} \qquad \ldots(33)^{\dagger}$$

$$+ \frac{\left(r_{Sn}^2 - r_{Bn}^2\right)\left(T_{Bn} + T_{Sn} - T_{B(n+1)} - T_{S(n+1)}\right)}{\frac{Z_{n+1}}{k_{n+1}} + \frac{Z_n}{k_n}} + 4k_nZ_n\left(T_{Bn} - T_{Cn}\right)$$

At the shield surface with subsequent radiation:

$$0 = \frac{Z_n\left(mr_{Sn}^2 + r_{Bn}^2(1 - m)\right)\left(T_{Sn} - T_{Bn}\right)}{\frac{m}{4k_n}\left(r_{Sn}^2 - r_{Bn}^2\right) + \frac{r_{Bn}^2}{2k_n}(m - 1)\,\ell n\,\frac{r_{Bn}}{r_{Sn}}} + 2\sigma\epsilon r_{Sn}Z_n\left(T_{Sn}^4 - T_A^4\right) \qquad \ldots(34)^{\dagger}$$

where

k_{n-1}, k_n, and k_{n+1} = the thermal conductivity of the nodes n, n+1, n-1, Btu/hr-ft-°F

Z_n = the thickness of the nodes, ft

T_{Cn}, T_{Bn}, and T_{Sn} = the central, thermal shield radius, and surface temperatures in n, °R

r_{Bn} = the thermal shield radius at n, ft

r_{Sn} = the outside radius of the shield at n, ft

---

†See Appendix D, Part III for the development of these equations.

ϵ = the emissivity at the surface

μ = lumped γ and n attenuation coefficient, ft^{-1}

T_A = the temperature of space, etc., °R

m = the ratio of the heat generation rate outside the thermal shield to that under the thermal shield

σ = the Stefan-Boltzman constant, 1.73×10^{-9} Btu/hr-ft^2 (°R)^4

Q_{oc} = the heat generation rate at the shield upper face, $\frac{Btu}{hr\text{-}ft^3}$

Equations 32, 33, and 34 may be applied to a shield divided into n axial nodes with the result being a series of simultaneous equations that may be solved with the aid of a computer.

NOMENCLATURE

A = surface area per fuel element, ft^2

a = coefficient in the hydrogen permeation equation, $(atm)^{-1}$

C = heat capacity, $\frac{Btu}{lb_m\text{-}°F}$

D = fuel element diameter, ft

E = Young's modulus, psi

G = mass flow rate of coolant, $\frac{lb_m}{hr\text{-}ft^2}$

h = heat transfer coefficient, $\frac{Btu}{hr\text{-}ft^2\text{-}°F}$

I = hot channel factor

k = thermal conductivity, $\frac{Btu}{hr\text{-}ft\text{-}°F}$

L = core length, ft

$\%L_H$ = % of hydrogen loss during reactor life

m = mass flow rate of coolant, $\frac{lb_m}{hr}$

N = hydrogen concentration in the fuel, $\frac{cc_{H_2}(STP)}{cc_{fuel}}$

n = number of fuel rods

n^1 = number of coolant channels

P = reactor power, $\frac{Btu}{hr}$

p = pressure, $\frac{lb_f}{in.^2}$

q = heat rate, $\frac{Btu}{hr}$

Q = volumetric heat generation rate, $\frac{Btu}{hr\text{-}ft^3}$

R = core radius (radius of a circle circumscribing the hexagon formed by the core), ft

also core radial coordinate

r = fuel rod radius, ft

S_o = hydrogen permeation rate at $T = \infty$, $\frac{cc(STP)}{hr\text{-}cm^2\text{-}atm}$

T = temperature, °F unless specified °R

t = time, hr

V_C = core volume, ft^3

X = thickness, ft

Y = yield strength, psi

Z = core axial coordinate

α = distance between adjacent fuel element centers/fuel element diameter

δ = fractional volume expansion

ΔE = "energy" associated with the hydrogen permeation process, °R

ϵ_C = coolant fraction in core

ϵ_f = fuel fraction in core

ϵ_s = solidity fraction of fuel elements in core

ν = Poisson's ratio

SUBSCRIPTS

c = cladding

e = equivalent

f = fuel

H = hydrogen gap

ht.ch. = hot channel

i = inlet

m = coolant

o = normal

P = power

s = coating

APPENDIX A
HEAT TRANSFER IN NONUNIFORMLY COOLED FUEL RODS

Appendix A demonstrates the derivations of the equations and methods used in determining the heat transfer in nonuniformly cooled fuel rods.

PART I
SOLUTION OF TEMPERATURE DISTRIBUTION IN NONUNIFORMLY COOLED CYLINDRICAL UNCLAD FUEL ELEMENT[7] (By R. L. Brehm)

A. ANALYSIS

The following assumptions are made in this analysis:

1) Steady-state conditions
2) The problem is two-dimensional
3) The volumetric heat generation is uniform over the element
4) The thermal conductivity of each region is constant
5) The element is divisible into an even number of equal circular sectors such that temperature symmetry exists between adjacent sectors.

The geometry of the problem is as shown in the sketch below. Region (1) represents the heat generation element and Region (2) the cladding. By assumption (5) no heat is transferred across either radial boundary. The heat transfer rates across the peripheries of the element and cladding are represented by $q_1(\theta)$ and $q_2(\theta)$ respectively.

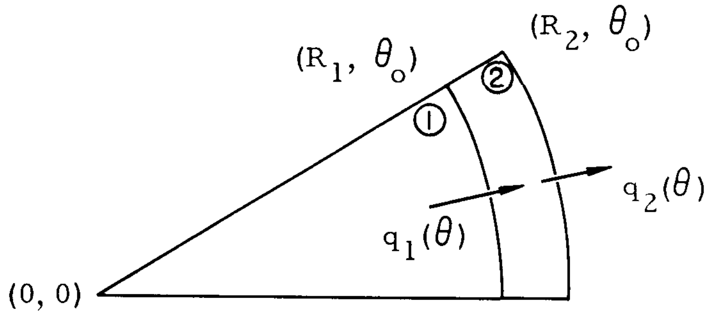

Solution for the Unclad Element:

Corresponding to the case of an unclad element, the solution for the temperature distribution in Region 1 will be determined in terms of $q_1(\theta)$.

The temperature in the element can be shown to satisfy Poisson's equation:

$$\frac{\partial^2 T_1}{\partial r^2} + \frac{1}{r}\frac{\partial T_1}{\partial r} + \frac{1}{r^2}\frac{\partial^2 T_1}{\partial \theta^2} + \frac{Q}{k_1} = 0 \qquad \ldots(A1)$$

with the boundary conditions:

1) $T_1(0,\theta) = T_o$

2) $\dfrac{\partial T_1(0,\theta)}{\partial r} = 0$

3) $k_1 \dfrac{\partial T_1(r, 0)}{\partial \theta} = 0$

4) $k_1 \dfrac{\partial T_1(r, \theta_o)}{\partial \theta} = 0$

5) $k_1 \dfrac{\partial T_1(R_1,\theta)}{\partial r} = -q_1(\theta)$

where $0 \le r \le R_1$ and $0 \le \theta \le \theta_o$.

The solution of Equation A1 is:

$$T_1(r,\theta) = U(r,\theta) - \frac{Q}{k_1}\frac{r^2}{4} \qquad \ldots(A2)$$

where $U(r,\theta)$ satisfies Laplace's equation

$$\frac{\partial^2 U}{\partial r^2} + \frac{1}{r}\frac{\partial U}{\partial r} + \frac{1}{r^2}\frac{\partial^2 U}{\partial \theta^2} = 0\ . \qquad \ldots(A3)$$

A solution of Equation A3 is:

$$U_n = a_o + b_o \ln r + \left(A_{\ell n} r^{\lambda_n} + A_{2n} r^{-\lambda_n}\right)\left(A_{3n} \sin\lambda_n\theta + A_{4n} \cos\lambda_n\theta\right) \qquad \ldots(A4)$$

where a_o, b_o, and λ_n are constants.

By applying boundary conditions (1), (2), and (3) Equation 4A is reduced to

$$U_n = a_o + A_{\ell n} A_{4n} r^{\lambda_n} \cos \lambda_n \theta \ .$$

Application of (4) determines the values of λ_n to be

$$\lambda_n = \frac{n\pi}{\theta_o} \qquad n = 1, 2, 3, \ldots$$

Defining

$$A_n = \frac{A_{\ell n} A_{4n}}{QR_1{}^2/k_1} R_1{}^{\lambda_n}$$

then

$$U_n = a_o + \frac{QR_1{}^2}{k_1} A_n \left(\frac{r}{R_1}\right)^{\lambda_n} \cos \lambda_n \theta \qquad \ldots (A5)$$

Since each U_n is a solution of Equation A3, the sum of all U_n's is also a solution. Hence,

$$T_1 = a_o - \frac{QR_1{}^2}{k_1}\left[\left(\frac{r}{2R_1}\right)^2 - \sum_{n=1}^{\infty} A_n \left(\frac{r}{R_1}\right)^{\lambda_n} \cos \lambda_n \theta\right] \ . \qquad \ldots (A6)$$

By (1), $a_o = T_o$

A nondimensional temperature, $T_1{}^*$, is now defined:

$$T_1{}^* = \frac{T_o - T_1}{QR_1{}^2/k_1} = \left[\left(\frac{r}{2R_1}\right)^2 - \sum_{n=1}^{\infty} A_n \left(\frac{r}{R_1}\right)^{\lambda_n} \cos \lambda_n\right] \qquad \ldots (A7)$$

Note that T_1^* is a function only of θ and the ratio r/R_1, i.e., T_1^* is a geometrical function independent of the thermal conductivity, the heat generation, or the size of the element.

To determine the coefficients A_n use is made of boundary condition (5) in the following manner. A dimensionless heat transfer rate, $q_1(\theta)$, is defined by

$$q_1^*(\theta) = \frac{q_1(\theta)}{QR_1} = R_1 \frac{\partial T_1^*(R_1, \theta)}{\partial r}$$

so that

$$q_1^*(\theta) = \frac{1}{2} - \sum_{n=1}^{\infty} \lambda_n A_n \cos \lambda_n \theta \; .$$

Multiplying both sides by $\cos \lambda_n$ and integrating from $-\theta_o$ to θ_o

$$A_n = -\frac{1}{\lambda_n \theta_o} \int_{-\theta_o}^{\theta_o} q_1^*(\theta) \cos \lambda_n \theta \, d\theta \qquad \ldots (A8)$$

where n = 1, 2, 3, ...

Thus, the temperature distribution in the unclad element is given by:

$$T_1^* = \left(\frac{r}{2R_1}\right)^2 + \sum_{n=1}^{\infty} \frac{1}{n\pi} \left(\frac{r}{R_1}\right)^{\frac{n\pi}{\theta_o}} \cos \frac{n\pi\theta}{\theta_o} \int_{-\theta_o}^{\theta_o} q_1^*(\theta) \cos \frac{n\pi}{\theta_o} \theta \, d\theta \qquad \ldots (A9)$$

NOMENCLATURE FOR APPENDIX A, PART I

A_i, B_i, C_i = i^{th} coefficients in series solutions

k_i = heat conductivity of i^{th} region

Q = volumetric heat generation rate

q_i = heat transfer rate across i^{th} peripheral boundary

q_i^* = nondimensional heat transfer rate, $\frac{q_i}{QR_1}$

R_i = outer radius of i^{th} region

T_i = temperature in i^{th} region

T_o = temperature at center of element (r = 0)

T_i^* = nondimensional temperature, $\frac{T_o - T_i}{QR_1{}^2/k_1}$

λ_i = i^{th} Eigen value

θ_o = sector angle

γ = ratio of thermal conductivities, $\frac{k_2}{k_1}$.

Other symbols are defined as used.

PART II

DERIVATION OF QUANTITIES USED IN THE DETERMINATION OF THE TEMPERATURE DISTRIBUTION FOR FUEL RODS IN A TRIANGULAR ARRAY[8,9] (By H. N. Rosenberg)

A. ROD TEMPERATURE

Consider three rods in a triangular array and the enclosed coolant channel. From symmetry, only the shaded portion in Figure A1 need be considered in the thermal analysis. Appendix A, Part I, has shown that the temperature distribution in a rod with uniform heat generation but asymmetrical heat removal may be given by Equation A9.

$$T_1^* = t^* = \left(\frac{r}{2R}\right)^2 + \sum_{n=1}^{\infty} \frac{2}{n\pi}\left(\frac{r}{R}\right)^{\frac{n\pi}{\theta_o}} \cos\frac{n\pi\theta}{\theta_o} \int_0^{\theta_o} q^*(\theta)\cos\frac{n\pi\theta}{\theta_o}\, d\theta \qquad \ldots (A10)$$

where

r = radius at a point

R = rod radius

θ_o = angle from hottest to coolest surface point

$q^* = \frac{q}{QR}$

q = heat flux

Q = volumetric heat generation rate

$t^* = \frac{t}{QR^2/k}$

t = center rod temperature minus temperature at a point

k = thermal conductivity of fuel

and where $\theta = 0$ at the point of close approach and $\theta = \theta_o$ at the cold point on the surface.

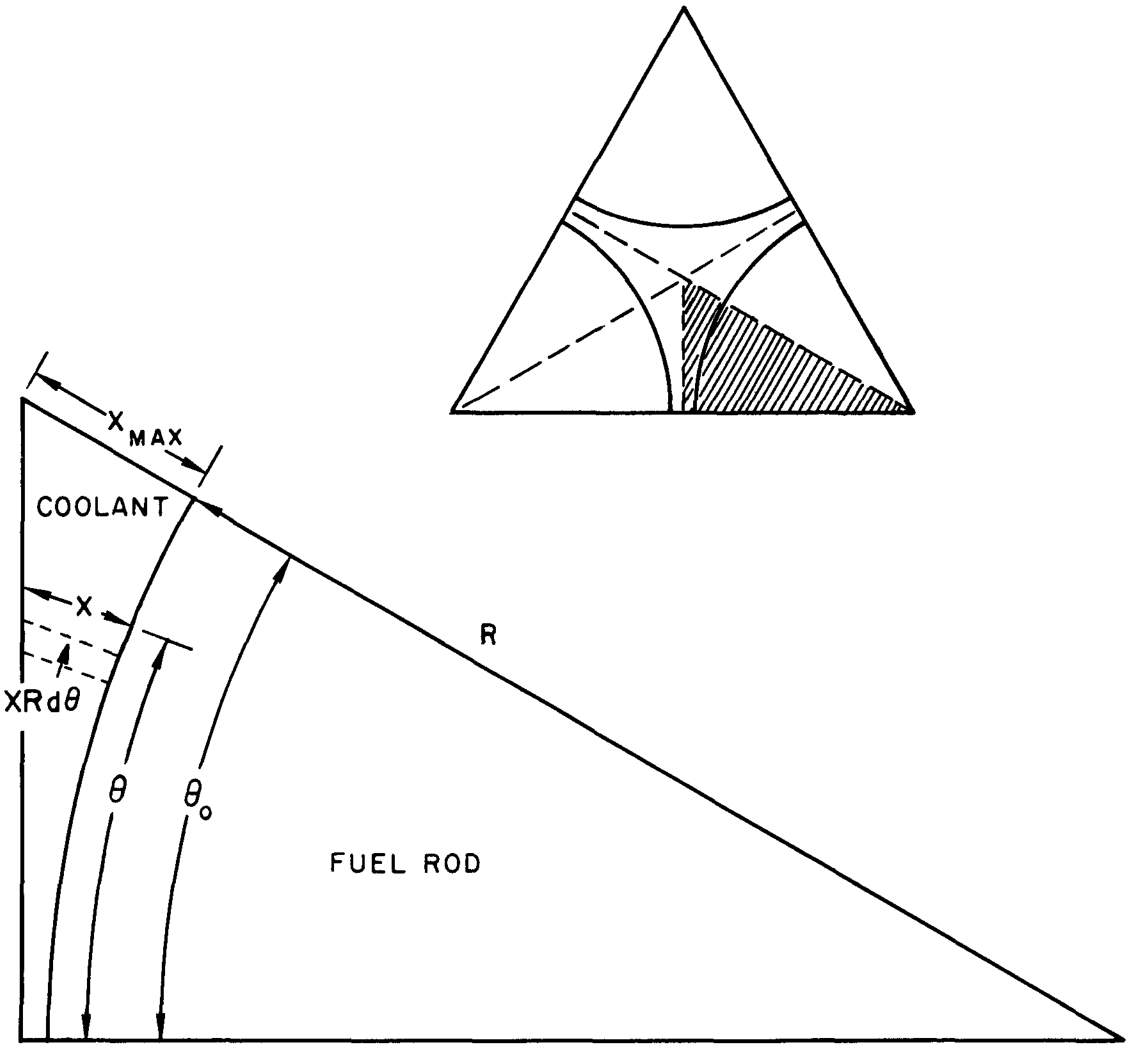

Figure A1. Flow Channel Cross Section

B. SURFACE HEAT FLUX DISTRIBUTION

The problem then is reduced to finding the heat removal distribution, $q^*(\theta)$, on the surface.

At this point we make the assumption that there is no flow of heat in the azimuthal direction in the coolant. The azimuthal flow of heat in the fuel alone is considered to generate the θ-dependence of temperature. The justifications for this assumption are three-fold.

1) In the important case of closely packed rods the cross-section for azimuthal heat flow in the coolant is small compared to the azimuthal heat flow area in the fuel. When the rods are far-spaced the azimuthal temperature gradient becomes small and the heat flow in that direction may still be neglected.
2) Where eddying is the major heat transport mechanism in the coolant, the fact that the velocity gradient is roughly perpendicular to the fuel surface (see Rosenberg[10] and Deissler and Taylor[11]), will cause the predominant heat flow to be radial in the channel.
3) In any case, ignoring azimuthal heat flow represents a conservative engineering assumption and will predict a higher hot spot temperature than will actually result.

Proceeding then, the heat flow at an angle θ will be equal to the heat removed by the coolant in the differential element $xRd\theta$ (see Figure A1). The heat removal rate, then, per length of channel in the differential area will be simply,

$$\rho C_p \frac{\partial T}{\partial z} u(\theta)x(\theta)Rd\theta \; . \qquad \ldots(A11)$$

The heat flux (heat per unit area of fuel surface) is then

$$q(\theta) = \rho C_p \frac{\partial T}{\partial z} u(\theta)x(\theta) \qquad \ldots(A12)$$

where

ρ = density of coolant

C_p = heat capacity of coolant

$\frac{\partial T}{\partial z}$ = temperature gradient in the axial direction

$u(\theta)$ = average velocity at the angle

$x(\theta)$ = channel width along a radius

If we make the customary assumption that $\frac{\partial T}{\partial z}$ is uniform over the channel and that ρ and C_p are independent of temperature, then the average heat flux over the fuel surface is

$$q_{av} = \frac{\rho C_p \frac{\partial T}{\partial z}}{\theta} \int_0^{\theta_o} u x d\theta \qquad \ldots(A13)$$

and, thus, the normalized heat flux is:

$$\epsilon(\theta) = \frac{q}{q_{av}} = \frac{ux}{\frac{1}{\theta_o}\int_0^{\theta_o} u x d\theta}. \qquad \ldots(A14)$$

Equation A14 may be rewritten,

$$\epsilon\left(\frac{\theta}{\theta_o}\right) = \frac{\left(\frac{u}{u_B}\right)\left(\frac{x}{x_{max}}\right)}{\int_0^1 \left(\frac{u}{u_B}\right)\left(\frac{x}{x_{max}}\right) d\left(\frac{\theta}{\theta_o}\right)} \qquad \ldots(A15)$$

where

u_B = bulk average velocity

x_{max} = value of x at θ_o

From Equation A15 it can be seen that the heat flux distribution $\epsilon(\theta/\theta_o)$ depends only on α, the pitch/diameter, since $\frac{x}{x_{max}}\left(\frac{\theta}{\theta_o}\right)$ depends only on α from geometrical considerations and $\frac{u}{u_B}\left(\frac{\theta}{\theta_o}\right)$ depends only on α from hydrodynamic considerations.

The average heat flux, q_{av}, is also equal to the heat generated in a rod divided by the surface area so that

$$q_{av} = \frac{QR}{2} \qquad \text{...(A16)}$$

and in Equation A10 then

$$q^* = \frac{q}{QR} = \frac{1}{2}\,\frac{q}{q_{av}} = \frac{\epsilon(\theta)}{2} \qquad \text{...(A17)}$$

The temperature distribution may be found then by substitution of the normalized heat flux distribution in Equation A10 if the velocity distribution $\frac{u}{u_B}\left(\frac{\theta}{\theta_o}\right)$ is known.

C. VELOCITY DISTRIBUTION

The velocity distribution for turbulent flow is obtained from the theoretical treatment of Deissler and Taylor.[11] The velocity distribution for laminar flow is obtained from the theoretical treatment[10] for touching rods with the use of an extrapolation technique to obtain the velocity distribution for separated rods.

The extrapolation is obtained thusly. Given a velocity distribution $\frac{u}{u_B}\left(\frac{\theta}{\theta_o}\right)$ for $\alpha = 1$, form the distribution $\frac{u}{u_B}\left(\frac{x}{x_{max}}\right)$. Then cut off the distribution at the minimum value of $\frac{x}{x_{max}}$ corresponding to a value of $\alpha = \alpha_1$ taking this to be the unnormalized $\frac{u}{u_B}\left(\frac{x}{x_{max}}\right)$ for α_1. The assumption then is that the velocity distribution depends only on $\frac{x}{x_{max}}$ in a channel. Notice that the laminar flow parameters in Figure A3 fall off in the same way as the turbulent parameters which used velocity distributions obtained from a detailed velocity mapping of the channel.

For the pitch/diameter, α_1, then an unnormalized $\frac{u}{u_B}\left(\frac{\theta}{\theta_o}\right)$ may be obtained and normalized to give the required velocity distribution.

D. DIMENSIONLESS PRESENTATION OF DATA

Note that t^* in Equation A10 is the actual center to point temperature difference divided by QR^2/k which is $4\Delta T_o$ where ΔT_o is the normal center to surface drop for no peripheral temperature variation ($\epsilon = 1$). The results are given for generality in terms of a fraction of ΔT_o.

As can be seen in Figures A2 and A3, the temperatures are related to the rod center temperature, T_o, as follows:

$$T_o - T_{max} = (1 - \gamma)\ T_o$$

$$T_o - T_{\infty} = \Delta T_o$$

$$T_o - T_{av} = (1 + \beta)\Delta T_o$$

$$T_o - T_{min} = (1 + \omega)\Delta T_o$$

where

T_{max} = maximum surface temperature (point of close approach)

T_{∞} = surface temperature for uniform surface heat flux

T_{av} = weighted average surface temperature according to quantity of adjacent fluid

$$T_{av} = \frac{\int_0^{\theta_o} T(R, \theta) x R d\theta}{\int_0^{\theta_o} x R d\theta}$$

T_{min} = minimum surface temperature

The weighted average surface temperature, T_{av}, is defined such that if there is negligible resistance to heat flow into the coolant, (large heat transfer coefficient) then T_{av} is the bulk coolant temperature. This is considered to be a good reference temperature for evaluating the effect of varying rod spacing.

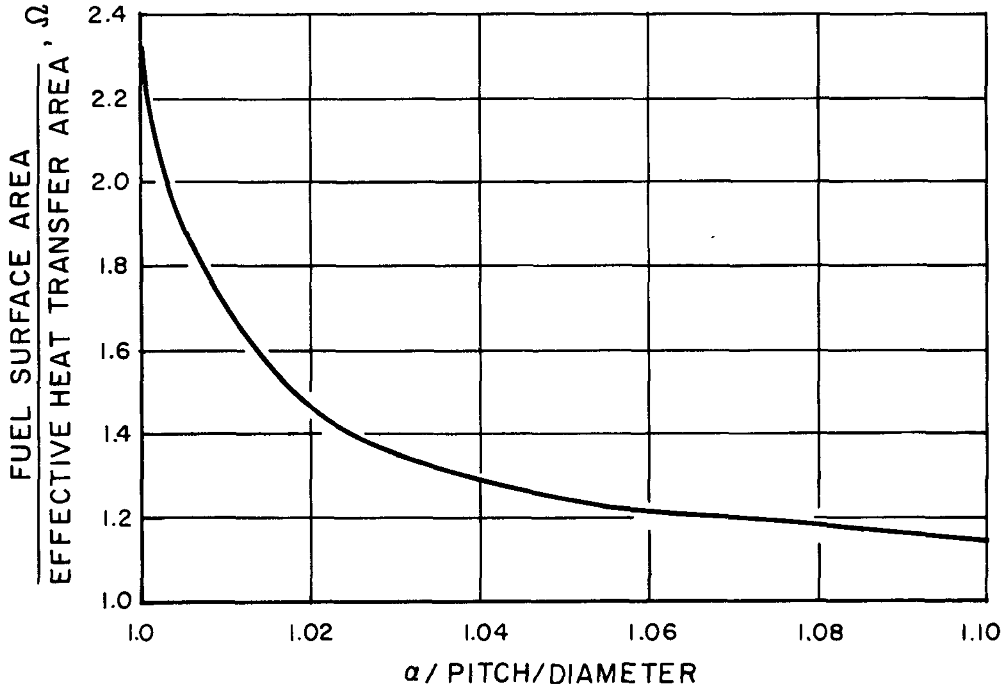

Figure A2. Effective Heat Transfer Area for Cladding, Coating, Hydrogen Gap, and Coolant Film

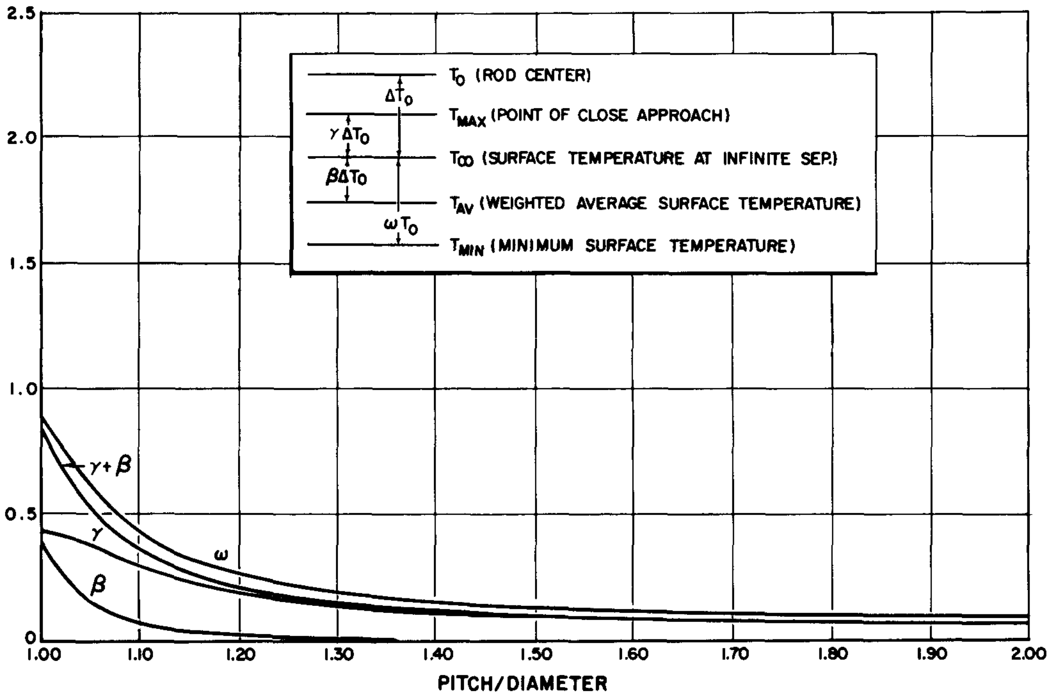

Figure A3. Parameters for Tricusp Channel Laminar Flow[9,10]

PART III

DETERMINATION OF THE EFFECT OF A TRICUSP CHANNEL ON HEAT TRANSFER THROUGH THE HYDROGEN GAP, COATING, CLADDING AND COOLANT FILM[1,2] (By P. D. Cohn)

Appendix A, Part II, has demonstrated a method for determining the heat transfer to a tricusp channel from a fuel rod with uniform heat generation. The quantity, Ω, is used to determine the effect of the tricusp channel on the heat transfer in the peripheral components of the fuel rods where Ω is defined as the fuel surface area divided by the heat transfer area in a close packed array. The nomenclature in this section is the same as in Appendix A. Part II.

$$\Omega = \frac{\Delta T}{\Delta T_\infty} = \frac{\text{temperature drop in close array}}{\text{temperature drop if rods are infinitely separated}}$$

$$\Omega = \frac{\displaystyle\int_0^{\theta_o} \frac{q(\theta)}{h} \frac{x}{x_{max}} \, d\left(\frac{\theta}{\theta_o}\right)}{\displaystyle\frac{q_{av}}{h} \int_0^{\theta_o} \frac{x}{x_{max}} \, d\left(\frac{\theta}{\theta_o}\right)} \qquad \ldots(A18\text{-}a)$$

$$\Omega = \frac{\displaystyle\int_0^{\theta_o} \frac{q(\theta)}{q_{av}} \frac{x}{x_{max}} \, d\left(\frac{\theta}{\theta_o}\right)}{\displaystyle\int_0^{\theta_o} \frac{x}{x_{max}} \, d\left(\frac{\theta}{\theta_o}\right)} \qquad \ldots(A18\text{-}b)$$

where x and θ are as shown in Figure A1, h is the heat transfer coefficient of the interface.

$$\frac{x}{x_{max}} = \frac{\dfrac{\alpha}{\cos\theta} - 1}{1.1547\alpha - 1} \qquad \alpha = \text{Pitch/Diameter} \qquad \ldots(A19)$$

Equation A19 may be evaluated by numerical methods using the data given in References 9 and 10.

Since $\Omega = \dfrac{\Delta T}{\Delta T_\infty}$, Ω may be reduced to $\dfrac{A_\infty}{A_{eff}}$. Figure A2, is a plot of Ω vs rod separation.

APPENDIX B
HYDROGEN LOSS AND REDISTRIBUTION

Appendix B presents the analytical solution of the hydrogen loss and redistribution equations.

PART I
SOLUTION OF THE HYDROGEN LOSS EQUATIONS[1,8,9]
(By P. D. Cohn and H. N. Rosenberg)

A. CALCULATION OF HYDROGEN LOSS

It has been determined by semi-empirical methods,[1] that hydrogen permeation through ceramics like the coating material is governed by Equation B1 which is basically the Langmuir equation[12] with an Arrhenius temperature dependence.

$$\phi_H = \frac{S_o P}{1 + aP} e^{-\overline{\Delta}E/T} \qquad \ldots (B1)$$

where

ϕ_H = hydrogen permeation rate $\frac{cc(STP)}{hr\text{-}cm^2}$

S_o = permeation rate at infinite temperature and is defined by the system, $\frac{cc(STP)}{hr\text{-}cm^2\text{-}atm}$

P = hydrogen pressure, atm

a = a constant determined by the system, 1/atm

$\overline{\Delta}E$ = $\Delta E/R$ where ΔE is the activation energy of the diffusion process and R is the universal gas constant in consistent units

T = coating temperature, °R

Applying Equation B1 to a reactor core

$$L_H = \frac{1}{V \epsilon_s} \int_0^t \int_A \frac{\phi_H}{N} \, dA dt \qquad \ldots (B2)$$

where

L_H = fraction of hydrogen lost

V = core volume, cm^3

ϵ_s = fuel fraction in core

t = time, hours

A = area for hydrogen leakage in core, cm^2

N = hydrogen concentration in core, $\frac{cc(STP)}{cc_{fuel}}$

If L_H is small, N is roughly constant with time, and Equation B2 may be rewritten:

$$L_H = \frac{t}{NV\epsilon_s}\int_A \phi_H dA \qquad \text{. . . (B3-a)}$$

or

$$L_H = \frac{tS_o}{NV\epsilon_s}\int_A \frac{P(z,r)}{1 + aP(z,r)} e^{-\overline{\Delta}E/T(z,r)} dA \qquad \text{. . . (B3-b)}$$

where the pressure and temperature variation over (z,r) is known. For a cylindrical reactor of height L, and assuming that T is invariant in r at constant height z, Equation B1 may be applied to the core configuration such that

$$\frac{\phi_H'}{\text{unit volume}} = t\int_0^1 \phi_H A_v d\left(\frac{z}{L}\right) \qquad \text{. . . (B4)}$$

where A_v/L = area/unit volume of core per unit length and ϕ_H' is the total hydrogen loss/unit volume in time t.

The fraction of hydrogen lost $L_H = \frac{\phi_H'}{\epsilon_s N}$, where $A_v = \frac{2\epsilon_s}{r}$

where

r = the fuel rod radius

L = the reactor length

Then

$$L_H = \frac{2t}{Nr}\int_0^1 \phi_H d\left(\frac{z}{L}\right) \qquad \ldots(B5)$$

Substituting for ϕ_H in Equation B5 and converting to % hydrogen loss,

$$\%L_H = \frac{200t}{Nr}\left(\frac{P}{1 + aP}\right)S_o \int_0^1 e^{-\overline{\Delta}E/T} d\left(\frac{z}{L}\right) \qquad \ldots(B6)$$

where P is the pressure due to the average fuel temperature and is the pressure throughout the rod.

If T may be linearized such that

$$T = T_i + \Delta T(z/L) \quad ,$$

then

$$\%L_H = \frac{200tS_o}{Nr}\left(\frac{P}{1 + aP}\right)\int_0^1 e^{-\overline{\Delta}E/\left[T_i + \Delta T(z/L)\right]} d\left(\frac{z}{L}\right) \qquad \ldots(B7)$$

Transforming by setting $(z/L) = (T - T_i)/(\Delta T)$, and defining a new variable $\mu = \overline{\Delta}E/T$, the integral in Equation B7 may be written as

$$\frac{\overline{\Delta}E}{T}\int_{\mu_1}^{\mu_2} \frac{e^{-\mu}}{\mu^2} d\mu \qquad \ldots(B8)$$

Equation B7 may then be integrated to yield:

$$\%L_{H_2} = \frac{200t\overline{\Delta}E}{Nr\Delta T}\left(\frac{P}{1 + aP}\right)\left[e^{-\mu}\left(\sum_{n=1}^{\infty}\frac{(-1)^n n!}{\mu^{(n+1)}}\right)\right]_{\mu = \overline{\Delta}E/T_i}^{\mu = \frac{\overline{\Delta}E}{T_i + \Delta T}} \qquad \ldots(B9)$$

PART II

SOLUTION OF THE HYDROGEN REDISTRIBUTION EQUATION[9]

(By H. N. Rosenberg)

A. METHOD OF CALCULATION

1. Heat of Transport Case

The flux $J[(g)/(cm^2 - sec)]$ of a species A in solution is given by irreversible thermodynamics as[13]

$$J = -DN\left(\frac{dN}{Ndy} + \frac{Q^*}{RT^2}\frac{dT}{dy}\right) \qquad \ldots(B10)$$

where

D = diffusion coefficient

N = concentration of A

y = length dimension

T = absolute temperature

R = universal gas content

Q^* = heat of transport

where the first term is the usual diffusion expression and the second term is the thermal diffusion contribution. Consider then the case where $J = 0$ which we shall call the Heat of Transport case. This corresponds to a rod with an impermeable surface bond on all surfaces and a temperature gradient in the axial direction only, or a rod with a radial temperature gradient only with impermeable bonding.

From Equation B10 with $J = 0$,

$$\frac{dN}{N} = -\frac{Q^* dT}{RT^2}\ , \qquad \ldots(B11)$$

since it may be assumed that Q^* is not a function of temperature or concentration.

This integrates to

$$N = C e^{Q^*/RT} \qquad \ldots(B12)$$

where from conservation of species A

$$C = \frac{N_o}{\int_0^1 e^{Q^*/RT} d\xi} \qquad \ldots (\mathrm{B13})$$

and

N_o = bulk average concentration of A

ξ = z/L for the axial case

$\xi = (r/R)^2$ for the radial case

z = axial dimension

L = axial extent

r = radial dimension

R = radial extent

Equation B13 can be numerically integrated for any arbitrary $T(\xi)$ and then the concentration profile is calculated from Equation B12.

The results can be somewhat simplified if we assume that

a) the variation in T is small, and
b) that $T \sim \xi$, i.e., $T = \Delta T \xi + T_1$

Both assumptions are well warranted in reactors. Examining Equation B13, the numerator may be written

$$\int_0^1 e^{Q^*/RT} d\xi = \frac{1}{\Delta T} \int_{T_1}^{T_2} e^{Q^*/RT} dT \qquad \ldots (\mathrm{B14})$$

For small variation in T

$$\frac{1}{\Delta T} \int_{T_1}^{T_2} - T^2 e^{Q^*/RT} d\left(\frac{1}{\Delta T}\right) = \frac{-T_{av}^2}{\Delta T} \int_{T_1}^{T_2} e^{Q^*/RT} d\left(\frac{1}{T}\right) \qquad \ldots (\mathrm{B15})$$

Integrating Equation B15

$$C = \frac{N_o \Delta T Q^*}{\left(RT_{av}^2\right)\left(e^{Q^*/RT_1} - e^{Q^*/RT_2}\right)} \qquad \ldots (\mathrm{B16})$$

The results can be put in a very simple form if we assume

a) the variation in T is small, and

b) the variation in N is small

From Equation B11, then

$$\frac{\Delta N}{N_o} = \frac{-Q^* \Delta T}{R T_{av}^2} \qquad \ldots (B17)$$

APPENDIX C
RADIATION DAMAGE AND THERMAL STRESS

PART I
SOLUTION OF EQUATION RELATING FUEL SWELLING AND RADIATION EFFECTS[1] (By P. D. Cohn)

Consider a fuel element containing fission gas bubbles in the form of equally distributed spheres all of which are the same size. The pressure developed in these spheres is

$$P = \frac{n_b RT}{V_b} \qquad \ldots (C1)$$

where

P = fission gas pressure
n_b = the moles of fission gas in the bubble
R = universal gas constant
T = absolute temperature
V_b = volume of the bubble

Since $V_b = \frac{4}{3}\pi r_b^3$ where r_b = radius of the bubble, then Equation C1 may be written:

$$P = \frac{3n_b RT}{4\pi r_b^3} \qquad \ldots (C2)$$

Let η = number of bubbles per cc of fuel. If m = g-moles of gas formed per fission and f = fissions per cc during the reactor life, then $(mf/\eta) = n_b$ = the number of g-moles of gas per bubble. Therefore, Equation C2 may be written as

$$P = \frac{3RmfT}{4\pi r_b^3 \eta} \qquad \ldots (C3)$$

If δ, the volume fraction change, is small, then

$$\delta = \frac{4}{3}\pi r_b^3 \eta \qquad \ldots (C4)$$

Substituting for $r_b^3 \eta$ in Equation C3

$$P = \frac{RmfT}{\delta} \qquad \ldots (C5)$$

For a thick walled sphere, subject to a uniform internal pressure P,

$$\sigma_{max} = \frac{3}{4} P \frac{c^3}{c^3 - r^3} \quad \text{Reference 14.} \qquad \ldots \text{(C6-a)}$$

if c >> r

where

r = internal radius, (r_b)

c = external radius, $(r_b + h)$ where h = wall thickness

Equation C6-a may be rewritten as:

$$\sigma_{max} = \frac{3}{4} P \frac{(r_b + h)^3}{(r_b + h)^3 - r_b^3} \qquad \ldots \text{(C6-b)}$$

or

$$\left(1 - \frac{r_b^3}{(r_b + h)^3}\right) \sigma_{max} = \frac{3}{4} P \qquad \ldots \text{(C6-c)}$$

$r_b^3/(r_b + h)^3$ may be written as a function of δ if some distribution of the concentric spheres denoted by r_b and $r_b + h$ is assumed since $r_b^3/(r_b + h)^3$ is the ratio of the bubble volume to the "stress sphere" volume.

If it is assumed that the bubble distribution in the fuel is in an array of equal volume cubes† δ may be related to the volume fraction, v_f, as:

$$v_f = \frac{\frac{4}{3}\pi r^3}{(2r)^3} = 0.524 \qquad \ldots \text{(C7)}$$

$$\therefore \quad \delta = \frac{0.524\, r_b^3}{(r_b + h)^3} \qquad \ldots \text{(C8)}$$

or

$$\frac{r_b^3}{(r_b + h)^3} = 1.91\,\delta \qquad \ldots \text{(C9)}$$

---

†This assumption is made so that Equation C6-c may be written as a function of δ. It will be shown that if δ is small, it is independent of the assumed distribution.

Equation C6-c may be written as

$$(1 - 1.915\delta)\sigma_{max} = \frac{3}{4}P \qquad \ldots(C10)$$

If the fuel is considered to be a perfectly brittle material, no volume deformation in the form of rupture or creep will take place until $\sigma_{max} = Y(T)$, the yield strength of the fuel at temperature T; and no deformation will take place after σ_{max} is relieved such that it is less than Y(T).

Equation C10 may be modified such that:

$$Y(T) = \frac{3}{4}\frac{P}{(1 - 1.91\delta)} \qquad \ldots(C11)$$

If P, as stated in Equation C5 is substituted in Equation C11,

$$\delta - 1.91\delta^2 = \frac{3RmfT}{4Y(T)} \qquad \ldots(C12)$$

If δ is small, $1.91\delta^2$ may be ignored and Equation C12 may be written as:

$$\delta = 0.75\frac{RmfT}{Y(T)} \qquad \ldots(C13)$$

Equation C13 may be seen to be independent of the bubble size, distribution, and density. m, the gram moles of fission gas produced per fission, may be assumed to be due to equilibrium halogens and noble gases only.

PART II

CALCULATION OF THERMAL STRESS

The maximum thermal stresses in a fuel rod with an (r,θ) temperature distribution are outlined here.

These stresses due to the radial temperature distributions are:[15]

$$\sigma_{rr} = \frac{E\alpha\gamma_o}{4(1 - \nu)}(a^2 - r^2) \qquad \ldots(C14)$$

$$\sigma_{\theta\theta} = \frac{E\alpha\gamma_o}{4(1 - \nu)}(a^2 - 3r^2) \qquad \ldots(C15)$$

$$\sigma_{zz} = \frac{E\alpha\gamma_o}{2(1-\nu)}(a^2 - 2r^2) - E\alpha\omega\gamma_o a^2 \qquad \ldots(C16)$$

where

E = modulus of elasticity
α = thermal expansion coefficient
ν = Poisson's ratio
γ_o = Q/4k at the point at highest power
Q = the volumetric heat generation rate
k = the thermal conductivity of the fuel
a = the fuel rod radius
ω = a function of the rod separation

The stress due to the θ temperature distribution is:

$$\sigma_{rr} = \sigma_{\theta\theta} = 0; \qquad \sigma_{zz} = -E\alpha\gamma_o r^2 \cos\theta \qquad \ldots(C17)$$

The maximum stress is in the axial direction and is greatest at $r = a$, $\theta = 0$. Combining Equations C16 and C17,

$$\sigma_{zz_{max}} = -E\alpha\gamma_o r^2 \left[1 + \omega + \frac{1}{2(1-\nu)}\right] . \qquad \ldots(C18)$$

APPENDIX D
RADIATION HEATING AND TEMPERATURE DETERMINATION IN COMPONENTS

This Appendix presents the development of the heat generation and temperature equations for radiation heating and temperature distribution in the reflector and shield.

PART I
RADIATION HEATING

The neutron heating in a material consisting of elements n, m, ... may be estimated in the following manner for thin members:

For heating due to neutron reaction in element n:

$$\frac{q_{nr}}{A} = \Sigma_{nr} \rho_n \phi(E_r) E_n V_n \qquad \ldots (D1)$$

where

$\frac{q_{nr}}{A}$ = energy due to the neutron - n reaction, $\frac{\text{mev}}{\text{sec-cm}^2}$

Σ_n = macroscopic cross section for the neutron reaction with element n, cm^{-1}

ρ_n = atom fraction of element in the material

$\phi(E)_r$ = neutron flux above the threshold energy for the reaction to take place, neutrons/cm^2-sec

E_n = energy produced in reaction, mev/neutron (this may be a fission as well as a simple nuclear reaction)

V_n = volume per unit area of material.

For energy deposition due to scattering:

$$\frac{q_{ns}}{A} = \rho_n \xi_n V_u \int_E \Sigma_{ns}(E)\phi(E) E dE \qquad \ldots (D2)$$

where

$\frac{q_{ns}}{A}$ = energy due to scattering process with element n

ξ_n = logarithmic energy decrement for material n

$\Sigma_{ns}(E)$ = macroscopic scattering cross section of n at energy E, cm^{-1}

$\phi(E)$ = neutron flux at energy E per unit energy, neutrons/cm^2-sec-mev.

$\int_E \Sigma_{ns}(E)\phi(E)dE$ may be evaluated in a step-wise manner using various intervals of E.

The total neutron heat flux is then:

$$q_{nr} + q_{ns} + q_{mr} + q_{ms} + \cdots = q_{neutron}$$

The energy deposited due to gammas may be calculated by: again in element n

$$\frac{q_{n}\gamma}{A} = \int_E e^{-\mu_c(E)t_c}\left[1 - e^{-\rho_n\mu_n(E)t_n}\right](E)dE \qquad \ldots(D3)$$

where

$\frac{q_n\gamma}{A}$ = energy dissipated in the material due to gamma interactions with element n

$\phi(E)$ = energy flux of gammas, mev/sec-cm^2 per mev interval

$\mu_c(E)$ = macroscopic gamma adsorption cross section at energy E for the core, cm^{-1}

t_c = characteristic distance that gammas must traverse through the core, cm

$\mu_n(E)$ = macroscopic energy cross section for material n, cm^{-1}

t_n = thickness of material containing element n, cm

Equation D3 may be evaluated by numerical methods.

The total heat generated, Q_B, in a thin member is simply the sum of the contributions of neutron reaction energy and energy due to gamma and neutron attenuation. For a thick member such as a shield, the effect of thickness must be taken into account. The heat generation due to radiation may be calculated when the attenuation coefficient, μ, for the radiation and material is known. This may be expressed by:

$$Q(x) = Q_{o\gamma} e^{-\mu_\gamma x} + Q_{on} e^{-\mu_n x} \qquad \ldots (D4)$$

where $Q_{o\gamma}$ and Q_{on} are the volumetric gamma and neutron heat generation rates at the interface and x is the axial extent.

PART II

CALCULATION OF REFLECTOR TEMPERATURES[6] (By P. D. Cohn)

The reflector temperatures may be calculated in the following manner, assuming that the reflector may be represented as:

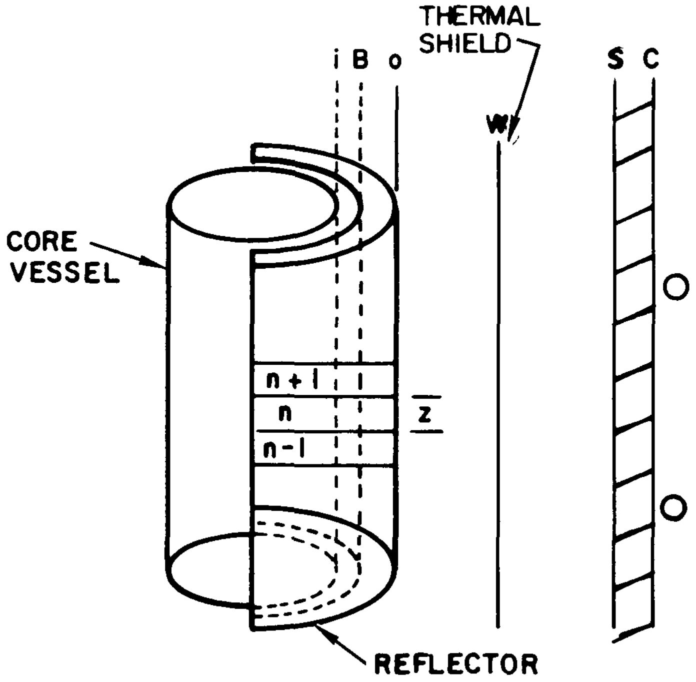

A heat balance is written around the reactor vessel-reflector interface with the resulting equations:

Considering radial and axial conduction in the reflector, and radiation and gas heat transfer at the reflector faces:

1) Heat transfer at the reactor - reflector interface at any axial interior node n:

$$Q_{in} = \sigma \epsilon_i A_i (T_{in}^4 - T_{Bn}^4) + hgA_i (T_{in} - T_{Bn}) \qquad \ldots \text{(D5)}$$

2) Axial and radial conduction in the reflector at any axial interior node n:

$$Q_{Bn} + Q_{in} = \frac{k}{x} \bar{A} (T_{Bn} - T_{on}) + \frac{nk}{Z} \frac{Az}{2} \left(2T_{Bn} - T_{B(n+1)} - T_{B(n-1)}\right) \qquad \ldots \text{(D6)}$$

3) Heat lost from the reflector exterior surface at any axial interior node n (to the atmosphere or space):

$$\frac{k}{x} \bar{A} (T_{Bn} - T_{on}) = \sigma \epsilon_o A_o (T_{on}^4 - T_A^4) + \frac{nk}{Z} \frac{Az}{2} \left(2T_{on} - T_{o(n-1)} - T_{o(n+1)}\right)$$

$$+ C_H A_o (T_{on} - T_A)^{1.25} \qquad \ldots \text{(D7)}$$

4) And adding the effect of heat transfer to the containment vessel cooling water:

$$\frac{1}{n} \sum_{1}^{n} (Q_i + Q_B)_n + Q_c = H_\omega A_\omega (T_\omega - T_c) \qquad \ldots \text{(D8)}$$

$T_A \simeq T_\omega$ for facility operation

where

Q_i = the thermal radiation heat transferred from the reactor vessel to the reflector, Btu/hr

Q_B = nuclear radiation heat rate, Btu/hr

σ = Stefan-Boltzman constant 1.73×10^{-9} Btu/hr-ft^2 (°R)^4

ϵ_i = emissivity at interface

ϵ_o = emissivity at beryllium surface

T_i = reactor coolant temperature at the core edge, °R

T_B = beryllium temperature at interface, °R

T_o = exterior beryllium temperature, °R

T_ω = temperature of wall in a facility, °R

A_i = area at reactor vessel reflector interface, ft^2

A = average area for heat conduction through beryllium, ft^2

A_o = area at reflector exterior, ft^2

k = thermal conductivity of beryllium, Btu/hr-ft-°F

x = beryllium thickness, ft

hg = gas heat transfer coefficient at reflector-reactor interface, Btu/hr-ft^2-°F

Z = node length in beryllium, ft

Az = annular area of beryllium cross section, ft^2

$C_H^{(3)}$ = gas heat transfer coefficient at reflector exterior surface, $\frac{\text{Btu}}{\text{hr-ft}^2\text{-°F}^{1.25}}$

n = number of nodes

Q_c = gamma and neutron heat generation in a pit liner (for facility operation), Btu/hr

A_ω = the wall area of containment vessel opposite reactor, ft^2

H_ω = the heat transfer coefficient of the wall, Btu/hr-ft^2-°F

T_c = cooling water temperature, °R

T_A = temperature of atmosphere or space, °R

The conservative assumption is made that all of the heat generated due to gamma and neutron heating is generated at the reactor vessel-reflector interface.

PART III
DETERMINATION OF SHIELD TEMPERATURES (By P. D. Cohn)

The following is a method by which the temperature distribution in a shield may be calculated.[1]

Assuming that the shield is essentially conical, it may be divided into regions such as:

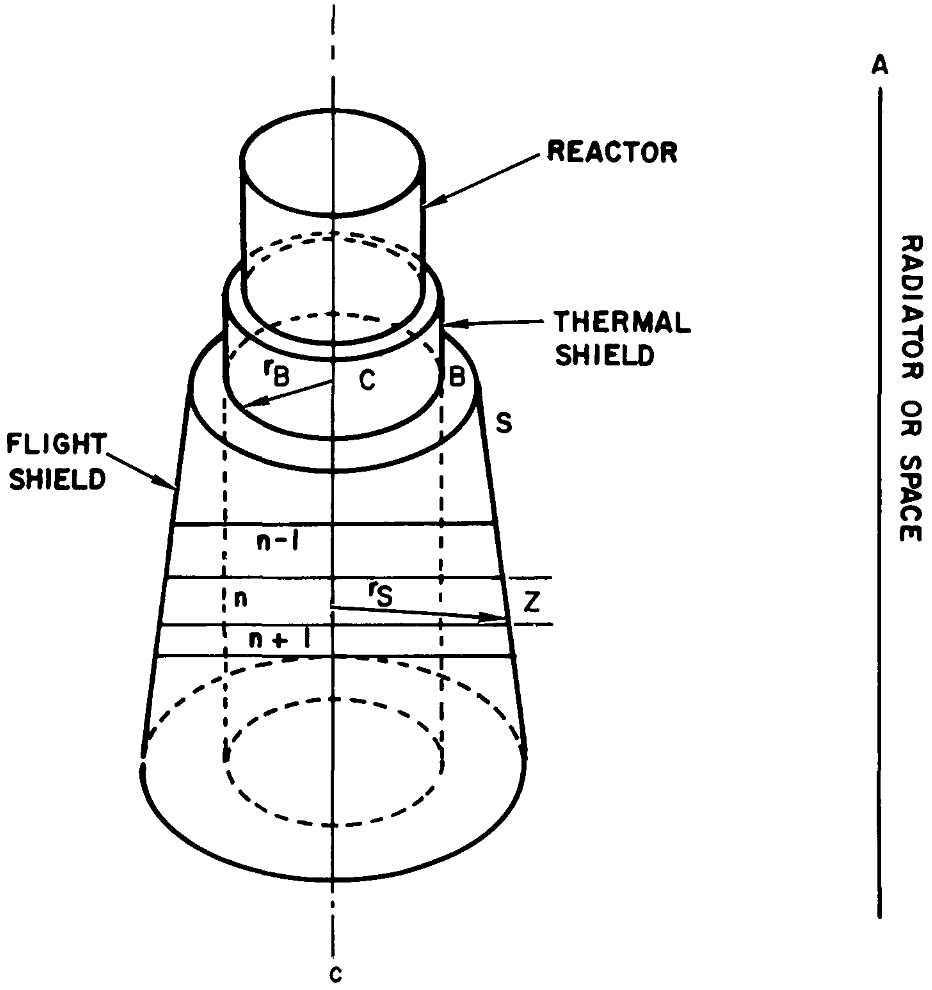

Power produced in Cn = P_{Cn}

C - B:

$$P_{Cn} = C_{Cn}(T_{Cn} - T_{Bn}) + C_{Cn, C(n-1)}\left(T_{Cn} - T_{C(n-1)}\right)$$

$$+ C_{Cn, C(n+1)}\left(T_{Cn} - T_{C(n+1)}\right) \qquad \ldots \text{(D9)}$$

B - S

$$P_{Bn} = C_{Bn}(T_{Bn} - T_{Sn}) + C_{Bn,\,B(n-1)}\left(T_{Bn} - T_{B(n-1)}\right)$$

$$+ C_{Bn,\,B(n+1)}\left(T_{Bn} - T_{B(n+1)}\right) + C_{Cn}(T_{Bn} - T_{Cn}) \qquad \ldots (D10)$$

At the surface:

$$0 = C_{Bn}(-T_{Bn} + T_{Sn}) + \sigma \epsilon A_n (T_{Sn}^4 - T_A^4) \qquad \ldots (D11)$$

where $A_n = 2 \; r_S Z_n$

For series conduction:

$$q_{n-1,\,n} = \frac{T_n - T_{n-1}}{\dfrac{Z_{n-1}}{2k_{n-1}} + \dfrac{Z_n}{2k_n}} \quad (A_C \text{ or } A_B) \qquad \ldots (D12)$$

where

$$A_C = \pi r_B^2$$

$$A_B = \pi (r_S^2 - r_B^2)$$

$\therefore$

$$C_{Cn,\,C(n-1)} = \frac{\pi r_B^2}{\dfrac{Z_{n-1}}{2k_{n-1}} + \dfrac{Z_n}{2k_n}} \; ; \; C_{Bn,\,B(n-1)} = \frac{\pi (r_S^2 - r_B^2)}{\dfrac{Z_{n-1}}{2k_{n-1}} + \dfrac{Z_n}{2k_n}}$$

and similarly for $C_{Cn,\,C(n+1)}$ and $C_{Bn,\,B(n+1)}$.

For uniform power generation:

C - B

$$Q_{Cn} = \frac{4k_n \Delta T_{Cn}}{r_B^2} \qquad \ldots(D13)$$

$$q_{Cn} = C_{Cn} \Delta T_{Cn} = Q_{Cn} V_{Cn} = Q_{Cn} \pi r_B^2 Z_n$$

$$q_{Cn} = \pi 4k_n \Delta T_{nC} Z_n$$

$$C_{Cn} = 4\pi k_n Z_n$$

For B - S:

$$\frac{d^2T}{dr^2} + \frac{1}{r}\frac{dT}{dr} = -\frac{Q}{k_n} \qquad \ldots(D14)$$

$$\frac{d}{dr}\left(r\frac{dT}{dr}\right) = -\, r\frac{Q}{k_n} \qquad \ldots(D15)$$

$$r\frac{dT}{dr} = -\frac{r^2}{2}\frac{Q}{k_n} + C_1 \qquad \ldots(D16)$$

$$\frac{dT}{dr} = -\frac{r}{2}\frac{Q}{k_n} + \frac{C_1}{r} \qquad \ldots(D17)$$

At $r = r_B$, $\frac{dT}{dr} = -\frac{Q_{Cn} V_{Cn}}{k_n A} = -\frac{Q_{Cn}}{2k_n}$,

$$\frac{C_1}{r_B} = -\frac{Q_{Cn} r_B}{2k_n} + \frac{r_B}{2}\frac{Q}{k_n} \; ; \quad C_1 = \frac{r_B^2}{2k_n}(Q - Q_{Cn})$$

$$dT = -\frac{r}{2}\frac{Q}{k_n}\,dr + \frac{1}{r}\,\frac{r_B^2}{2k_n}(Q - Q_{Cn})\,dr \qquad \ldots(D18)$$

$$T = -\frac{Qr^2}{4k_n} + \frac{r_B^2}{2k_n}(Q - Q_{Cn})\,\ell n r + C_2 \qquad \ldots(D19)$$

$$\text{At } r = r_S,\; T = T_o = -\frac{Qr_S^2}{4k_n} + \frac{r_B^2}{2k_n}(Q - Q_{Cn})\,\ell n r_S + C_2 \qquad \ldots(D20)$$

$$C_2 = T_o + \frac{Qr_S^2}{4k_n} - \frac{r_B^2}{2k_n}(Q - Q_{Cn})\,\ell n r_S$$

$$T - T_o = \Delta T = -\frac{Qr^2}{4k_n} + \frac{Qr_S^2}{4k_n} + \frac{r_B^2}{2k_n}(Q - Q_{Cn})\,\ell n \frac{r}{r_s} \qquad \ldots(D21)$$

$$\Delta T\Big|_{r=r_B} = \frac{Q}{4k_n}(r_S^2 - r_B^2) + \frac{r_B^2}{2k_n}(Q - Q_{Cn})\,\ell n \frac{r_B}{r_S} \qquad \ldots(D22)$$

Let $Q = Q_{Bn}$.

It is known that $$Q_{Bn} = mQ_{Cn}$$

$$Q_{Bn} - Q_{Cn} = Q_{Cn}(m-1)$$

$$\Delta T\Big|_{r=r_B} = \frac{mQ_{Cn}}{4k_n}\left(r_S^2 - r_B^2\right) + \frac{r_B^2}{2k_n}Q_{Cn}(m - 1)\ell n \frac{r_B}{r_S} \qquad \ldots(D23)$$

Considering the shield equations:

$$q_{Bn} = C_{Bn}\Delta T_{Bn} = mQ_{Cn}V_{Bn} + Q_{Cn}V_{Cn}$$

$$q_{Bn} = \frac{\pi\Delta T_{Bn}Z_n\left(mr_S^2 + (m - 1)\,r_B^2\right)}{\frac{m}{4k_n}\left(r_S^2 - r_B^2\right) + \frac{r_B^2}{2k_n}(m - 1)\,\ell n \frac{r_B}{r_S}} \qquad \ldots(D24)$$

∴

$$C_{Bn} = \frac{\pi Z_n\left(m r_S^2 + (m - 1) r_B^2\right)}{\frac{m}{4k_n}\left(r_S^2 - r_B^2\right) + \frac{r_B^2}{2k_n}(m - 1)\ln\frac{r_B}{r_S}}$$

$$q_{Cn} = Q_{Cn} r_{Cn} = Q_{Cn}\pi r_B^2 Z_n = Q_{oc}\pi r_B^2 Z_n\, e^{-\mu Z_n(n-1)} = P_{Cn}$$

$$q_{Bn} = mQ_{Cn} r_{Bn} = mQ_{oc}\pi Z_n\left(r_S^2 - r_B^2\right) e^{-\mu Z_n(n-1)} = P_{Bn}$$

Inserting the appropriate constants for node Cn in Equation D9:

$$Q_{oc} r_{Bn} Z_n\, e^{-\mu Z_n(n-1)} = 4k_n Z_n(T_{Cn} - T_{Bn}) + \frac{2r_{Bn}^2\left(T_{Cn} - T_{C(n-1)}\right)}{\frac{Z_{n-1}}{k_{n-1}} + \frac{Z_n}{k_n}}$$

$$+ \frac{2r_{Bn}^2\left(T_{Cn} - T_{C(n+1)}\right)}{\frac{Z_{n+1}}{k_{n+1}} + \frac{Z_n}{k_n}} \qquad \text{...(D25)}$$

Inserting the appropriate constants for node Bn in Equation D10 and distributing the axial heat conduction between T_{Bn} and T_{Sn}: At B:

$$mQ_{oc} Z_n\ r_{Sn}^2 - r_{Bn}^2\ e^{-\mu Z_n(n-1)} = \frac{Z_n\left(m r_{Sn}^2 + r_{Bn}^2(1 - m)\right)\left(T_{Bn} - T_{Sn}\right)}{\frac{m}{4k_n}\left(r_{Sn}^2 - r_{Bn}^2\right) + \frac{r_{Bn}^2}{2k_n}(m - 1)\ln\frac{r_{Bn}}{r_{Sn}}}$$

$$+ \frac{\left(r_{Sn}^2 - r_{Bn}^2\right)\left(T_{Bn} + T_{Sn} - T_{B(n-1)} - T_{S(n-1)}\right)}{\frac{Z_{n-1}}{k_{n-1}} + \frac{Z_n}{k_n}} \qquad \text{...(D26)}$$

$$+ \frac{\left(r_{Sn}^2 - r_{Bn}^2\right)\left(T_{Bn} + T_{Sn} - T_{B(n+1)} - T_{S(n+1)}\right)}{\frac{Z_{n+1}}{k_{n+1}} + \frac{Z_n}{k_n}} + 4k_n Z_n(T_{Bn} - T_{Cn})$$

At the surface S:

$$0 = \frac{Z_n\left(m r_{Sn}^2 + r_{Bn}^2 (1 - m)\right)\left(T_{Sn} - T_{Bn}\right)}{\frac{m}{4k_n}\left(r_{Sn}^2 - r_{Bn}^2\right) + \frac{r_{Bn}^2}{2k_n}(m - 1)\,\ell n\,\frac{r_{Bn}}{r_{Sn}}} + 2\sigma\epsilon\, r_{Sn} Z_n \left(T_{Sn}^4 - T_A^4\right) \qquad \ldots(D27)$$

This derivation to approximate the shield temperature distribution has been shown to have a deviation of 2.5% from a more exact digital solution.[16]

REFERENCES

1. P. D. Cohn, Unpublished Data, Atomics International, Canoga Park, Calif.
2. H. N. Rosenberg, Editor, "SNAP 8 Reactor Preliminary Design Summary," NAA-SR-6207, April 5, 1961.
3. Chemical Engineers Handbook, 3rd Ed., p 388.
4. A. W. Sommer, Unpublished Data, Atomics International, Canoga Park, Calif.
5. C. E. Ells, "Chalk River Report," PR-CM-13, 1958.
6. R. B. Hinze, "Design of the SNAP 8 Experimental Reactor," to be published, Canoga Park, Calif.
7. R. L. Brehm, Unpublished Data, Atomics International, Canoga Park, Calif.
8. F. H. S. Clark, Jr. III, "Analysis of S-2-DR Design," NAA-SR-5890.
9. H. N. Rosenberg, Unpublished Data, Atomics International, Canoga Park, Calif.
10. H. N. Rosenberg, Trans. Am. Nuclear Society, December 1958, Paper No. 7-6.
11. R. Deissler and M. Taylor, Reactor Heat Transfer Conference of 1956, TID-7529, Book 2.
12. W. K. Lewis, L. Squires, and G. Broughton, Industrial Chemistry of Colloidal and Amorphous Materials, The MacMillan Co., 1954.
13. Markowitz and Belle, WAPD TM-42, 1957.
14. R. J. Roark, Formulas for Stress and Strain, p 276, McGraw-Hill Book Company, 1954.
15. H. L. Sujata, Unpublished Data, Atomics International, Canoga Park, Calif.
16. R. D. Elliott, Unpublished Data, Atomics International, Canoga Park, Calif.